An enriched finite element for the simplified stress analysis of an entire bonded overlap: continuum macro-element

Sébastien Schwartz, Eric Paroissien, Frédéric Lachaud

An enriched finite element for the simplified stress analysis of an entire bonded overlap: continuum macro-element

Sébastien Schwartz[a,*], Éric Paroissien[a], Frédéric Lachaud[a]

[a] *Institut Clément Ader, Université de Toulouse, ISAE-SUPAERO, INSA, IMT MINES ALBI, UTIII, CNRS, 3 Rue Caroline Aigle, Toulouse, 31400, France*

Abstract

A methodology for the formulation of the stiffness matrix of an enriched finite element, called continuum macro-element (CME), representing for the full length of a bonded overlap and both the adhesive and the adhesive in only one four-node elements, is presented. Compared to earlier macro-elements modelling the bonded overlap as beams on elastic foundation, the CME supposed the adherends and the adhesive as plane continuum media, for which higher-order displacement fields is supposed for the adhesive. The formulation of the stiffness matrix for the adherend outside of the overlap is presented as well to address the stress analysis of single-lap bonded joint for assessment purpose. The assessment is performed by comparisons with the results from (i) a plane strain finite element and (ii) two recent papers by Nguyen and Le Grognec [1] and Methfessel and Becker [2]. Good agreements are shown.

Keywords: Macro-element, Continuum element, 2D element, Single Lap Joint, Simplified stress analysis

*Corresponding author
Email address: sebastien.schwartz@isae-supaero.fr (Sébastien Schwartz)
URL: https://github.com/sschwart/research (Sébastien Schwartz)

1. Introduction

The sizing of structural adhesively bonded joints is currently subjected to investigations by research teams worldwide. The sizing process mainly consists in comparing design values to criteria; the design values are measured thanks to experimental tests, while the criteria need the assessment of suitable mechanical fields provided by a stress analysis. Detailed finite element (FE) analyses can address the stress analysis of bonded joints. Nevertheless, these detailed FE analyses can be costly in terms of preprocessing, computation and postprocessing, so that simplified stress analyses providing accurate results are attractive.
In 1909, Arnovljevic [3] developed a model for a composite bar made of a pipe filled by a rod axially loaded. The pipe and the rod are joined all over their contact surface. The load transfer between the pipe and the rod is performed at the interface through a shear stress supposed to be proportional to the relative displacement at the interface: a shear-lag approach. The model aimed at assessing the maximal sustainable load as a function of the shear strength of the interface. In 1938, Volkersen [4] provided a model for the stress analysis of single-lap bonded joint in-plane loaded, the objective of which was to assess the load transfer distribution within a bonded joint. In this model, both adherends are seen as bars and the load transfer is performed by shearing the adhesive layer, assuming a shear stress proportional to the relative displacement of adherends at the interface. These first models consider then the adherends as bars linked by a bed of shear springs, allowing for the load transfer, by the adhesive layer in the case of the model by Volkersen. It comes that the system of ordinary differential equations (ODE) to solve is only dependent on the adherend longitudinal displacements, which are coupled through the stiffness associated to the adhesive. In other words, the local equilibrium of the adhesive layer is not considered. This modelling approach includes the models based on beams or plate on elastic foundation: the Volkersen model is based on bars on one-parameter foundations. In this paper, this type of model is called discrete model, since the load transfer is ensured by the deformation of discrete elements: the springs representing for the adhesive layer. The stress analysis developed in 1944 by Goland and Reissner [5] is a discrete model (plate on two-parameters elastic foundation) for which the bending of adherends, non-linearly dependent on the in-plane tensile force due to the neutral line lag, is considered as well as the associated adhesive peel stress. The discrete model by Goland and Reissner has then been enriched by modifying the simplifying hypotheses, in terms of local equilibrium equations of adherends and kinematics for the adhesive and adherends by several authors such as for example Hart-Smith [6], Ojalvo et Eidinoff [7], Oplinger [8] or Luo and Tong [9, 10, 11]. It is indicated that the previous models provide closed-form ready-to-use solutions, valid on a restricted application field in terms of boundary conditions and nature of joined materials. To overcome the restriction due to the boundary conditions, stress analyses of the bonded overlap only were developed and are referred to sandwich type analyses [12, 13, 14, 15, 16]. The loading applied on the adherends at overlap ends, in terms of force and/or displacement, is supposed to be known. Moreover, depending on the constitutive equations of joined adherends, the governing system of ODEs can show a coupling level leading to the necessary use of a computer program to assess the roots and integration constants. Some authors suggested simplification reducing the level of coupling even for sandwich type analysis [13, 17]. In particular, the discrete model by Zhao et al. [17] involves adherends modeled as plane stress or plane stain continuum

media. Finally, to extend the application field of discrete models to various geometrical configurations under various boundary conditions and loadings, including nonlinear material behaviors, dedicated resolution schemes were developed such the approach by Mortensen et al. [18, 19] based on the multi-segment integration scheme or the macro-element (ME) modelling by Paroissien et al. [20, 21]. A ME is representing both the adherends and the adhesive layer in one four-nodes FE with one or three degrees of freedom (DoF) per node depending on the kinematics chosen for the adherends. The interpolation functions are not supposed a priori but take the shape of the solution of the governing system of ODEs, so that only one ME is sufficient to represent for the entire bonded overlap: discretization is not necessary for a linear material computation. The ME results in the computation of the stiffness matrix K, similar to elementary stiffness matrix from finite element (FE) theory. Therefore, it could be possible to compute existing capabilities from FE theory such as the consideration of non-linear law behaviour. A second category of simplified stress analyses can gather the models which consider the local equilibrium equations for the adhesive layer. In this paper, this type of models is called continuum model. These models do not lead to parametrical closed-form ready-to-use equations and need a computer program to assess the roots and integration constants [22, 23, 24, 25], eventually associated with a dedicated resolution scheme [26, 27]. Recently, Nguyen and Le Grognec [1] or Methfessel and Becker [2] published models involving higher-order displacement approaches associated with a dedicated resolution scheme. Particularly, Nguyen and Le Grognec formulated an enriched FE representing both adherends and the adhesive layer in one FE, similarly to the ME. This enriched FE is a three-nodes FE element with nine DoF per node and using a quadratic interpolation and a discretization of the overlap is need to assess the mechanical answer.
During the last decade, different methodologies for the formulation of stiffness and mass matrices of ME have been developed to allow for the enrichment of MEs, modelling a bonded – eventually multi-layered – overlap [20, 28, 21, 29, 30]. However, all these methodologies consider discrete MEs (DME) only. The objective of this paper is to present a methodology for the formulation of a stiffness matrix of a continuum ME (CME) based on higher-order displacement approach along the y-axis and to be able to represent an entire bonded overlap. The enriched CME approach give to a structure designed with it, a quick access to the longitudinal, transversal/shear and peel stresses along the x-axis and y-axis, thanks to its FE-similarities, without meshing part. The adherends and the adhesive are regarded as plane strain or stress continuum media under small displacements and with a linear elastic material behaviour. The case of a non-linear geometry behaviour and non-linear material behaviour, such as plasticity or damage, are not considered. No crack or failure are considered. The adherends are considered under the first-order shear deformation while the adhesive kinematics is assumed to follow a second and third-order description for axial and transversal displacement. The CME is assessed by comparing the predicted adhesive stress distributions with those provided by a refined plane strain FE model and by two recent paper models: (i) Nguyen and Le Grognec [1] and (ii) by Methfessel and Becker [2].

2. Formulation of continuum macro-element

2.1. Underlying assumptions

In order to keep the model simple, some assumptions are taken and provided in this section. Materials are assumed to be homogeneous and isotropic. The considered behavior is linear elastic, with a Young's modulus E_i and a Poisson's coefficient ν_i. The subscript i refers either to the adhesive (denoted "a") or to an adherend i where $i = 1$ for the upper adherend and $i = 2$ for the lower adherend (see Figure 1). The material is seen as a 2D continuous solid (in the xy-plane) with the possibility to satisfy the plane stress or the plane strain hypothesis. Therefore $E_i^{'}$, $G_i^{'}$ and $\nu_i^{'}$ are used for general formulation, and can be expressed as:

- Plane stress:

$$\left| \begin{array}{l} E_i^{'} = E_i \\ G_i^{'} = G_i \\ \nu_i^{'} = \nu_i \end{array} \right. \tag{1}$$

- Plane strain:

$$\left| \begin{array}{l} E_i^{'} = \frac{E_i}{1-\nu_i^2} \\ G_i^{'} = G_i \\ \nu_i^{'} = \frac{\nu_i}{1-\nu_i} \end{array} \right. \tag{2}$$

Two type of ME have been developed and described in the following sections. The first ME is a beam that represents the full length l_i of the adherend "i". The width is quoted b. The stiffness matrix of this element will be usefull to model the SLJ with MEs (see Section 3). The second ME is the CME that represents the full length L of the bonded overlap made of both adherends "i" and of the adhesive "a" whom the thickness are $2h_i$ with $i = 1, 2, a$. The width is quoted b as well.
For both previous MEs, the adherends are considered under the first-order shear deformation. The adhesive kinematics is assumed to follow a second and third-order description for axial and transversal displacement. Finally, the loading is considered to be quasi-static and small strain and displacements are considered.

2.2. Virtual work principle

The virtual work principal is used to produce a set of equilibrium equations [31] as:

$$\delta W = \delta W_{int} + \delta W_{ext} = 0 \quad \forall \delta U_1, \delta U_2, \delta U_a \tag{3}$$

where δU_1, δU_2 and δU_a are considered as kinematically admissible and as the virtual variations of the unknown displacement fields U_1, U_2 and U_a, in the upper/lower substrate and in the adhesive layer. The variational internal and external work are respectively denoted δW_{int} and δW_{ext}. For the current problem, the first variation of the internal (i.e. strain) energy $\delta W_{int,i}$ of an element i is written as:

$$\delta W_{int,i} = -\int_{\Omega_i} \delta\varepsilon_i^T \sigma_i \, d\Omega_i = -\int_{\Omega_i} \delta\varepsilon_{i,xx}\sigma_{i,xx} + \delta\varepsilon_{i,yy}\sigma_{i,yy} + \delta\varepsilon_{i,xy}\sigma_{i,xy} \, d\Omega_i \tag{4}$$

where Ω_i, $\delta\varepsilon_i^T$ and σ_i are respectively the volume, the variational strain and the stress.

2.3. Adherend component

The upper and lower adherends are considered under the first-order shear deformation. The general displacement field is composed of a longitudinal and a transversal displacement of the centroïd axis, respectively noted $u_i(x)$ and $v_i(x)$, and the rotation $\theta_i(x)$ of its section around the z-axis. The general displacement field U_i of this beam for an element subscript i is:

$$U_i(x,y) = \left| \begin{array}{l} u_i(x) + \theta_i(x).y \\ v_i(x) \end{array} \right. \tag{5}$$

The strain vector of an element i is:

$$\varepsilon_i = \begin{bmatrix} \varepsilon_{i,xx} \\ \varepsilon_{i,yy} \\ 2\varepsilon_{i,xy} \end{bmatrix} = \begin{bmatrix} \frac{du_i(x)}{dx} + \frac{d\theta_i(x)}{dx}.y \\ 0 \\ \frac{dv_i(x)}{dx} + \theta_i(x) \end{bmatrix} \tag{6}$$

From the Hooke's Law, the stress vector can be computed as:

$$\sigma_i = \begin{bmatrix} \sigma_{i,xx} \\ \sigma_{i,yy} \\ \sigma_{i,xy} \end{bmatrix} = \begin{bmatrix} E_i^{'} & \nu_i^{'}E_i^{'} & 0 \\ \nu_i^{'}E_i^{'} & E_i^{'} & 0 \\ 0 & 0 & G_i^{'} \end{bmatrix} \begin{bmatrix} \varepsilon_{i,xx} \\ \varepsilon_{i,yy} \\ 2\varepsilon_{i,xy} \end{bmatrix} \tag{7}$$

$$\sigma_i = \begin{bmatrix} E_i^{'}\left(\varepsilon_{i,xx} + \nu_i{'}\varepsilon_{i,yy}\right) \\ E_i^{'}\left(\nu'\varepsilon_{i,xx} + \varepsilon_{i,yy}\right) \\ 2G_i^{'}\varepsilon_{i,xy} \end{bmatrix} = \begin{bmatrix} E_i^{'}\frac{du_i(x)}{dx} + E_i^{'}\frac{d\theta_i(x)}{dx}y \\ E_i^{'}\nu'\frac{du_i(x)}{dx} + E_i^{'}\nu_i{'}\frac{d\theta_i(x)}{dx}y \\ G_i^{'}\left(\frac{dv_i(x)}{dx} + \theta_i(x)\right) \end{bmatrix} \tag{8}$$

By considering the variational form of Eq. 6 and performing integration by parts on the derivative of the displacement $\delta u_i(x)$, $\delta v_i(x)$, and $\delta\theta_i(x)$, to have them without derivation, Eq. 4 can be written as:

$$\begin{aligned} \delta W_{int,i} &= -\int_{\Omega_i} \delta\varepsilon_{i,xx}\sigma_{i,xx} + \delta\varepsilon_{i,xy}\sigma_{i,xy}\, d\Omega_i \\ &= -\int_{\Omega_i} \frac{d\delta u_i(x)}{dx}.\sigma_{i,xx} + \frac{d\delta\theta_i(x)}{dx}y.\sigma_{i,xx} + \frac{d\delta v_i(x)}{dx}\sigma_{i,xy} + \delta\theta_i(x)\sigma_{i,xy}\, d\Omega_i \\ &= \int_{l_i} \delta u_i(x)\frac{dN_{i,xx}}{dx} + \delta\theta_i(x)\left(\frac{dM_{i,zz}}{dx} - N_{i,xy}\right) + \delta v_i(x)\frac{dN_{i,xy}}{dx}\, dx \\ &- \left[\delta u_i(x)N_{i,xx} + \delta\theta_i(x)M_{i,zz} + \delta v_i(x)N_{i,xy}\right]_0^{l_i} \end{aligned} \tag{9}$$

with

$$N_{i,xx} = \int_{S_i} \sigma_{i,xx}\, dS_i \qquad M_{i,zz} = \int_{S_i} y.\sigma_{i,xx}\, dS_i \qquad N_{i,xy} = \int_{S_i} \sigma_{i,xy}\, dS_i \tag{10}$$

where l_i and S_i are respectively the longitudinal length and the transversal surface of an element i.

2.4. Adhesive component

For the adhesive, the displacement field is defined through a polynomial series in terms of y-coordinate. The general displacement field for the adhesive a is assumed to be written under the following shape:

$$U_a(x,y) = \left| \begin{array}{l} \sum_{i=0}^{n} u_i^a(x)\, y^i \\ \sum_{i=0}^{m} v_i^a(x)\, y^i \end{array} \right. \tag{11}$$

Due to the polynomial shape along the y-axis of the displacement field, it is possible to have a good agreement of the physical behavior by choosing the right couple (n, m). According to [1], in order to have a proper stress and strain distribution through the thickness, it is proposed to take $n = 2$ and $m = 3$, leading to the following expression:

$$U_a(x,y) = \left| \begin{array}{l} u_0^a(x) + u_1^a(x).y + u_2^a(x).y^2 \\ v_0^a(x) + v_1^a(x).y + v_2^a(x).y^2 + v_3^a(x).y^3 \end{array} \right. \tag{12}$$

The strain vector is then deduced such as:

$$\varepsilon_a = \begin{bmatrix} \frac{du_0^a(x)}{dx} + \frac{du_1^a(x)}{dx}.y + \frac{du_2^a(x)}{dx}.y^2 \\ v_1^a(x) + 2v_2^a(x).y + 3v_3^a(x).y^2 \\ \left(u_1^a(x) + \frac{dv_0^a(x)}{dx}\right) + \left(2u_2^a(x) + \frac{dv_1^a(x)}{dx}\right) y + \frac{dv_2^a(x)}{dx}.y^2 + \frac{dv_3^a(x)}{dx}.y^3 \end{bmatrix} \tag{13}$$

From the Hooke's Law (see Eq. 7), the stress vector is computed as:

$$\sigma_a = \begin{bmatrix} E_a' \left(\frac{du_0^a(x)}{dx} + \nu_a' v_1^a(x)\right) + E_a' \left(\frac{du_1^a(x)}{dx} + 2\nu_a' v_2^a(x)\right) y + E_a' \left(\frac{du_2^a(x)}{dx} + 3\nu_a' v_3^a(x)\right) y^2 \\ E_a' \left(\nu_a' \frac{du_0^a(x)}{dx} + v_1^a(x)\right) + E_a' \left(\nu_a' \frac{du_1^a(x)}{dx} + 2v_2^a(x)\right) y + E_a' \left(\nu_a' \frac{du_2^a(x)}{dx} + 3v_3^a(x)\right) y^2 \\ G_a' \left(u_1^a(x) + \frac{dv_0^a(x)}{dx}\right) + G_a' \left(2u_2^a(x) + \frac{dv_1^a(x)}{dx}\right) y + G_a' \frac{dv_2^a(x)}{dx}.y^2 + G_a' \frac{dv_3^a(x)}{dx}.y^3 \end{bmatrix} \tag{14}$$

By considering the variational form of Eq. 13, Eq. 4 can be written as:

$$\begin{aligned} \delta W_{int,a} = -\int_{\Omega_i} & \frac{d\delta u_0^a(x)}{dx}.\sigma_{a,xx} + \frac{d\delta u_1^a(x)}{dx} y.\sigma_{a,xx} + \frac{\delta u_2^a(x)}{dx}.y^2\sigma_{a,xx} \\ & + \delta v_1^a(x)\sigma_{a,yy} + 2\delta v_2^a(x).y\sigma_{a,yy} + 3\delta v_3^a(x).y^2\sigma_{a,yy} \\ & + \left(\delta u_1^a(x) + \frac{d\delta v_0^a(x)}{dx}\right)\sigma_{a,xy} + \left(2\delta u_2^a(x) + \frac{d\delta v_1^a(x)}{dx}\right) y\sigma_{a,xy} \\ & + \frac{d\delta v_2^a(x)}{dx}.y^2\sigma_{a,xy} + \frac{d\delta v_3^a(x)}{dx}.y^3\sigma_{a,xy}\, d\Omega_i \end{aligned} \tag{15}$$

For simplification purpose, the following expressions are considered:

$$\begin{aligned} N_{a,xx} &= \int_{S_a} \sigma_{a,xx}\, dS_a \qquad & M_{a,xx,n} &= \int_{S_a} y^n.\sigma_{a,xx}\, dS_a \\ N_{a,yy} &= \int_{S_a} \sigma_{a,yy}\, dS_a \qquad & M_{a,yy,n} &= \int_{S_a} y^n.\sigma_{a,yy}\, dS_a \\ N_{a,xy} &= \int_{S_a} \sigma_{a,xy}\, dS_a \qquad & M_{a,xy,n} &= \int_{S_a} y^n.\sigma_{a,xy}\, dS_a \end{aligned} \tag{16}$$

where l_a and S_a are respectively the longitudinal length and the transversal surface of the adhesive a. By using Eq. 16 and performing integration by parts on the derivative of the displacement $\delta u_0^a(x)$, $\delta u_1^a(x)$, $\delta u_2^a(x)$, $\delta v_0^a(x)$, $\delta v_1^a(x)$, $\delta v_2^a(x)$, and $\delta v_3^a(x)$, to have them without derivation, Eq. 15 can be simplified in:

$$\begin{aligned}\delta W_{int,a} = \int_{l_a} & \delta u_0^a(x)\frac{dN_{a,xx}}{dx} + \delta u_1^a(x)\left(\frac{dM_{a,xx,1}}{dx} - N_{a,xy}\right) \\ & + \delta u_2^a(x)\left(\frac{dM_{a,xx,2}}{dx} - 2M_{a,xy,1}\right) + \delta v_0^a(x)\frac{dN_{a,xy}}{dx} \\ & + \delta v_1^a(x)\left(\frac{dM_{a,xy,1}}{dx} - N_{a,yy}\right) + \delta v_2^a(x)\left(\frac{dM_{a,xy,2}}{dx} - 2M_{a,yy,1}\right) \\ & + \delta v_3^a(x)\left(\frac{dM_{a,xy,3}}{dx} - 3M_{a,yy,2}\right) dx \\ & - [\delta u_0^a(x)N_{a,xx} + \delta u_1^a(x)M_{a,xx,1} + \delta u_2^a(x)M_{a,xx,2} + \delta v_0^a(x)N_{a,xy} \\ & + \delta v_1^a(x)M_{a,xy,1} + \delta v_2^a(x)M_{a,xy,2} + \delta v_3^a(x)M_{a,xy,3}]_0^L\end{aligned} \tag{17}$$

2.5. Governing equations

To determine the stiffness matrix of the adherend without adhesive and the stiffness matrix of the macro-element representing the entire bonded overlap made of both adherends and of the adhesive, a set of ODEs needs to be established and be solved. To obtain this set, the virtual work principal presented in Section 2.2 is used, where Eq. 3 with the kinematically admissible field leads to the constrain that each term of the sum of Eq. 4 needs to be null.

2.5.1. Adherend without adhesive

Starting from Eq. 3, the set of ODEs for an adherend i without adhesive comes from:

$$\delta W_{int,i} + \delta W_{ext} = 0 \quad \forall \delta u_i(x), \delta v_i(x), \delta \theta_i(x) \tag{18}$$

The substitution of Eq. 9 into Eq. 18 results in the following set of ODEs:

$$\begin{cases} \dfrac{dN_{i,xx}}{dx} = 0 \\ \dfrac{dM_{i,zz}}{dx} - N_{i,xy} = 0 \\ \dfrac{dN_{i,xy}}{dx} = 0 \end{cases} \tag{19}$$

with:

$$\begin{cases} N_{i,xx} = 2bh_i E_i' \dfrac{du_i(x)}{dx} \\ N_{i,xy} = 2bh_i G_i' \left(\dfrac{dv_i(x)}{dx} + \theta_i(x)\right) \\ M_{i,zz} = \dfrac{2}{3} bh_i^3 E_i' \dfrac{d\theta_i(x)}{dx} \end{cases} \tag{20}$$

2.5.2. Bonded part

The adherends are modeled as in Section 2.3, and the adhesive part as in Section 2.4. Starting from Eq. 3, the set of ODEs comes from:

$$\begin{aligned}&\delta W_{int,1} + \delta W_{int,a} + \delta W_{int,2} + \delta W_{ext} = 0\\&\forall \delta u_0^a(x), \delta u_1(x), \delta\theta_1(x), \delta u_2(x), \delta\theta_2(x), \delta v_0^a(x), \delta v_1^a(x), \delta v_1(x), \delta v_2(x)\end{aligned} \tag{21}$$

The displacement fields are continuous at the interface adherend to adhesive, so that the following equations hold:

$$\begin{aligned}U_1(x, y = -h_1) &= U_a(x, y = h_a)\\U_2(x, y = h_2) &= U_a(x, y = -h_a)\end{aligned} \tag{22}$$

The insertion of Eq. 5 and Eq. 12 in Eq. 22 leads to:

$$\begin{aligned}u_1^a(x) &= -\frac{h_2}{2h_a}\theta_2(x) - \frac{h_1}{2h_a}\theta_1(x) - \frac{1}{2h_a}u_2(x) + \frac{1}{2h_a}u_1(x)\\u_2^a(x) &= \frac{h_2}{2h_a^2}\theta_2(x) - \frac{h_1}{2h_a^2}\theta_1(x) - \frac{1}{h_a^2}u_0^a(x) + \frac{1}{2h_a^2}u_2(x) + \frac{1}{2h_a^2}u_1(x)\\v_2^a(x) &= \frac{1}{2h_a^2}v_2(x) + \frac{1}{2h_a^2}v_1(x) - \frac{1}{h_a^2}v_0^a(x)\\v_3^a(x) &= -\frac{1}{h_a^2}v_1^a(x) - \frac{1}{2h_a^3}v_2(x) + \frac{1}{2h_a^3}v_1(x)\end{aligned} \tag{23}$$

By inserting Eq. 23 into Eq. 9 and Eq. 17, and using them into Eq. 21, it leads to the following set of ODEs:

$$\begin{cases}\dfrac{dN_{a,xx}}{dx} - \dfrac{1}{h_a^2}\left(\dfrac{dM_{a,xx,2}}{dx} - 2M_{a,xy,1}\right) = 0\\\dfrac{dN_{1,xx}}{dx} + \dfrac{1}{2h_a}\left(\dfrac{dM_{a,xx,1}}{dx} - N_{a,xy}\right) + \dfrac{1}{2h_a^2}\left(\dfrac{dM_{a,xx,2}}{dx} - 2M_{a,xy,1}\right) = 0\\\dfrac{dN_{2,xx}}{dx} - \dfrac{1}{2h_a}\left(\dfrac{dM_{a,xx,1}}{dx} - N_{a,xy}\right) + \dfrac{1}{2h_a^2}\left(\dfrac{dM_{a,xx,2}}{dx} - 2M_{a,xy,1}\right) = 0\\\dfrac{dM_{1,zz}}{dx} - N_{1,xy} - \dfrac{h_1}{2h_a}\left(\dfrac{dM_{a,xx,1}}{dx} - N_{a,xy}\right) - \dfrac{h_1}{2h_a^2}\left(\dfrac{dM_{a,xx,2}}{dx} - 2M_{a,xy,1}\right) = 0\\\dfrac{dM_{2,zz}}{dx} - N_{2,xy} - \dfrac{h_2}{2h_a}\left(\dfrac{dM_{a,xx,1}}{dx} - N_{a,xy}\right) + \dfrac{h_2}{2h_a^2}\left(\dfrac{dM_{a,xx,2}}{dx} - 2M_{a,xy,1}\right) = 0\\\dfrac{dN_{a,xy}}{dx} - \dfrac{1}{h_a^2}\left(\dfrac{dM_{a,xy,2}}{dx} - 2M_{a,yy,1}\right) = 0\\\dfrac{dM_{a,xy,1}}{dx} - N_{a,yy} - \dfrac{1}{h_a^2}\left(\dfrac{dM_{a,xy,3}}{dx} - 3M_{a,yy,2}\right) = 0\\\dfrac{dN_{1,xy}}{dx} + \dfrac{1}{2h_a^2}\left(\dfrac{dM_{a,xy,2}}{dx} - 2M_{a,yy,1}\right) + \dfrac{1}{2h_a^3}\left(\dfrac{dM_{a,xy,3}}{dx} - 3M_{a,yy,2}\right) = 0\\\dfrac{dN_{2,xy}}{dx} + \dfrac{1}{2h_a^2}\left(\dfrac{dM_{a,xy,2}}{dx} - 2M_{a,yy,1}\right) - \dfrac{1}{2h_a^3}\left(\dfrac{dM_{a,xy,3}}{dx} - 3M_{a,yy,2}\right) = 0\end{cases} \tag{24}$$

with:

$$\begin{cases} N_{a,xx} = 2bh_a E_a^{'} \left(\dfrac{du_0^a(x)}{dx} + {\nu_a}' v_1^a(x) \right) + \dfrac{2}{3} bh_a^3 E_a^{'} \left(\dfrac{du_2^a(x)}{dx} + 3{\nu_a}' v_3^a(x) \right) \\ M_{a,xx,1} = \dfrac{2}{3} bh_a^3 E_a^{'} \left(\dfrac{du_1^a(x)}{dx} + 2{\nu_a}' v_2^a(x) \right) \\ M_{a,xx,2} = \dfrac{2}{3} bh_a^3 E_a^{'} \left(\dfrac{du_0^a(x)}{dx} + {\nu_a}' v_1^a(x) \right) + \dfrac{2}{5} bh_a^5 E_a^{'} \left(\dfrac{du_2^a(x)}{dx} + 3{\nu_a}' v_3^a(x) \right) \end{cases} \tag{25}$$

$$\begin{cases} N_{a,yy} = 2bh_a E_a^{'} \left({\nu_a}' \dfrac{du_0^a(x)}{dx} + v_1^a(x) \right) + \dfrac{2}{3} bh_a^3 E_a^{'} \left({\nu_a}' \dfrac{du_2^a(x)}{dx} + 3v_3^a(x) \right) \\ M_{a,yy,1} = \dfrac{2}{3} bh_a^3 E_a^{'} \left({\nu_a}' \dfrac{du_1^a(x)}{dx} + 2v_2^a(x) \right) \\ M_{a,yy,2} = \dfrac{2}{3} bh_a^3 E_a^{'} \left({\nu_a}' \dfrac{du_0^a(x)}{dx} + v_1^a(x) \right) + \dfrac{2}{5} bh_a^5 E_a^{'} \left({\nu_a}' \dfrac{du_2^a(x)}{dx} + 3v_3^a(x) \right) \end{cases} \tag{26}$$

$$\begin{cases} N_{a,xy} = 2bh_a G_a^{'} \left(u_1^a(x) + \dfrac{dv_0^a(x)}{dx} \right) + \dfrac{2}{3} bh_a^3 G_a^{'} \dfrac{dv_2^a(x)}{dx} . y^2 \\ M_{a,xy,1} = \dfrac{2}{3} bh_a^3 G_a^{'} \left(2u_2^a(x) + \dfrac{dv_1^a(x)}{dx} \right) + \dfrac{2}{5} bh_a^5 G_a^{'} \dfrac{dv_3^a(x)}{dx} \\ M_{a,xy,2} = \dfrac{2}{3} bh_a^3 G_a^{'} \left(u_1^a(x) + \dfrac{dv_0^a(x)}{dx} \right) + \dfrac{2}{5} bh_a^5 G_a^{'} \dfrac{dv_2^a(x)}{dx} \\ M_{a,xy,3} = \dfrac{2}{5} bh_a^5 G_a^{'} \left(2u_2^a(x) + \dfrac{dv_1^a(x)}{dx} \right) + \dfrac{2}{7} bh_a^7 G_a^{'} \dfrac{dv_3^a(x)}{dx} \end{cases} \tag{27}$$

The expression of $N_{i,xx}$, $N_{i,xy}$ and $M_{i,zz}$ with $i \in [1, 2]$ are obtained from Eq. 20.

2.6. Stiffness matrix

To compute the stiffness matrix of the adherend without adhesive (see Section 2.3) and the stiffness matrix of the bonded part (see Section 2.4), the system of ODEs (respectively Eq. 19-20 and Eq. 24-25) need to be independently solved through a matrix formulation. The matrix representation is a powerful tool to manage complex systems of ODEs. A set of ODEs can be rewritten under the matrix form as:

$$\frac{dY(x)}{dx} = A.Y(x) \tag{28}$$

where A is a squared matrix. This matrix is provided in Appendix A.2 for the adherend i only and for the bonded part case. The vector Y and its derivative are:

$$\begin{aligned} Y(x) &= \begin{bmatrix} q(x) & \frac{dq(x)}{dx} \end{bmatrix}^T \\ \frac{dY(x)}{dx} &= \begin{bmatrix} \frac{dq(x)}{dx} & \frac{d^2q(x)}{dx^2} \end{bmatrix}^T \end{aligned} \tag{29}$$

where the superscript T indicates the transposition of a vector. The vector $q(x)$ is expressed as:

$$\begin{cases} q(x) = \begin{bmatrix} u_i(x) & v_i(x) & \theta_i(x) \end{bmatrix} \\ \rightarrow \text{for the adherend } i \in [1,2] \text{ (see Section 2.5.1)} \\ q(x) = \begin{bmatrix} u_0^a(x) & u_1(x) & \theta_1(x) & u_2(x) & \theta_2(x) & v_0^a(x) & v_1^a(x) & v_1(x) & v_2(x) \end{bmatrix} \\ \rightarrow \text{for the CME (see Section 2.5.2)} \end{cases} \tag{30}$$

A well-known solution of this differential equation is:

$$Y(x) = e^{A.x}.C \tag{31}$$

where C is the vector of unknown integration constants. The adherend and the CME have respectively 6 and 18 unknown integration constants. The matrix exponential can be computed manually using the Jordan approach as in [29], or using the built-in function of calculus software. The last approach is retained. The vector $q(x)$ (see Eq. 30) can be extracted from the vector $Y(x)$, allowing to expression the displacement field at any point x.
Using the resulting vector $q(x)$, the nodal displacement vector U and the nodal force vector F can be respectively expressed in term of integration constants as $U = D.C$ and $F = L.C$ where D and L are squared matrices. For each macro-element, the displacement and loading vector U and F are detailed in Appendix A.1. Finally, the stiffness matrix K is computed as $K = L.D^{-1}$ [21, 29, 30].

3. Validation

3.1. Case study

In the present paper, a focus is given on the SLJ configuration. The SLJ configuration (see Figure 1) has a depth b (i.e. in the z-direction) and both adherends (denoted "1" for the upper and "2" for the lower adherend) are considered to eventually be dissimilar. The length of overlap region (i.e. along the x-axis) is termed L and the length of the out-bonded part (i.e. part without adhesive) are respectively termed l_1 and l_2 for the upper and lower adherends. The thickness of the adhesive (i.e. along the y-axis) is $2h_a$ and for the upper and lower adherend, they are respectively termed $2h_1$ and $2h_2$. The adherends have the same

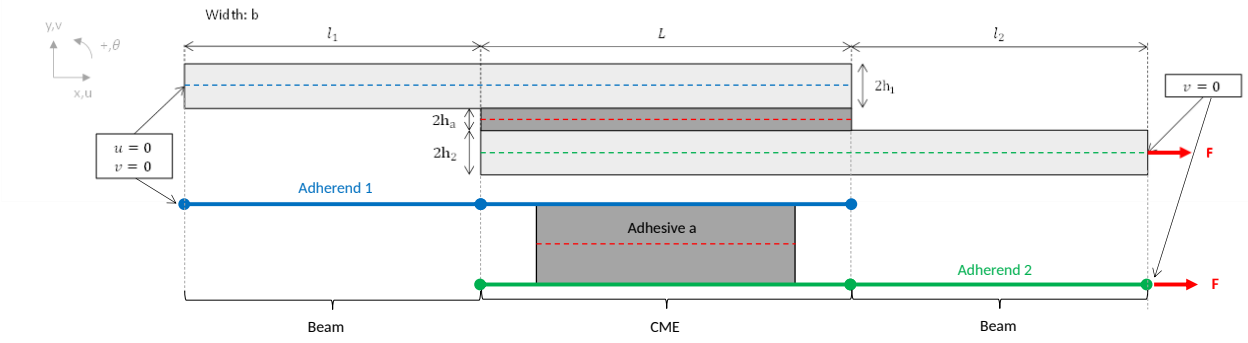

Figure 1: Representation of a Single Lap Joint (SLJ) and its modeling using macro-elements

geometry and material properties. The SLJ is simply supported and under a quasi static

force loading F. With the hypothesis of having a linear geometric behavior, the solicitation leads to small displacements. Material properties and geometric parameters used are given in each dedicated subsection.
The SLJ can be divided into three parts. Each part are modeled with only one ME, resulting in a total of three MEs to represent the SLJ configuration. From Section 2.6, the stiffness matrices for the adherend part without adhesive and for the bonded part is computed and are then assembled to represent the SLJ geometry (see Figure 1) such as in the traditional FE theory. With this modeling, it is possible to have the same advantages than with the FE theory, such as flexibility on boundary conditions and on the loading. The minimization of the potential energy lead to the classical linear system $F_S = K_S.U_S$ is then solved, where F_S and U_S are respectively the vector of nodal forces and nodal displacements of the structure which as a stiffness matrix K_S.
The proposed model is compared against a 2D FE model using the commercial FE codes SAMCEF/SIEMENS on the SLJ configuration, and against two recent analytical models, (1) Nguyen and Le Grognec model in 2021 [1] and (2) Methfessel and Becker model in 2022 [2].

3.2. 2D finite element model

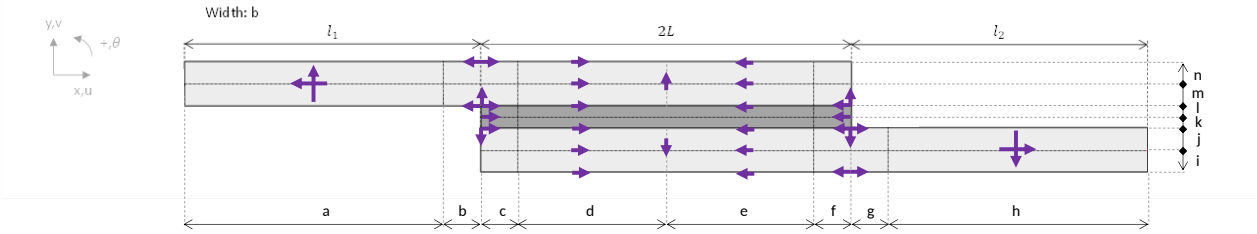

Figure 2: Mesh strategy for the SLJ geometry

The SLJ geometry is meshed with 4-nodes linear element, two degrees of freedom per node under normal integration and plane-strain assumption. To decrease the number of nodes and elements while keeping accuracy, a mesh strategy has been established. As shown in Figure 2, the SLJ geometry has been divided into several meshing domains. The FE mesh is distributed with a ration of 5 following the arrows, where the arrow direction provides the monotonic growth of the mesh, in Figure 2. An aspect and an transition ratio both equal to 1 are considered. Thus, the free overlap edges (i.e. at $x = 0$ and $x = L$) are meshed of squared through the adhesive thickness. The final results is visible on Figure 3 and related parameters are given in Table 1. The geometric and material parameters considered are respectfully detailed in Table 2 and Table 3. A load F of 100 N/mm is applied. In Figure 4, the variation of the maximal mid-plane adhesive stresses are provided in function of the number of elements in the adhesive thickness. The model is then considered to be converged at around 8 elements in the thickness. For precision, the model with 12 elements is retained. The distributions of the adhesive stresses along the mid-plane (i.e. $y = 0$) and the lower interface (i.e. $y = -h_a$) of the adhesive layer are provided in Figure 5 and Figure 6 respectively for the FE and the ME model. The longitudinal (σ_{xx}), transverse/peel (σ_{yy}), and

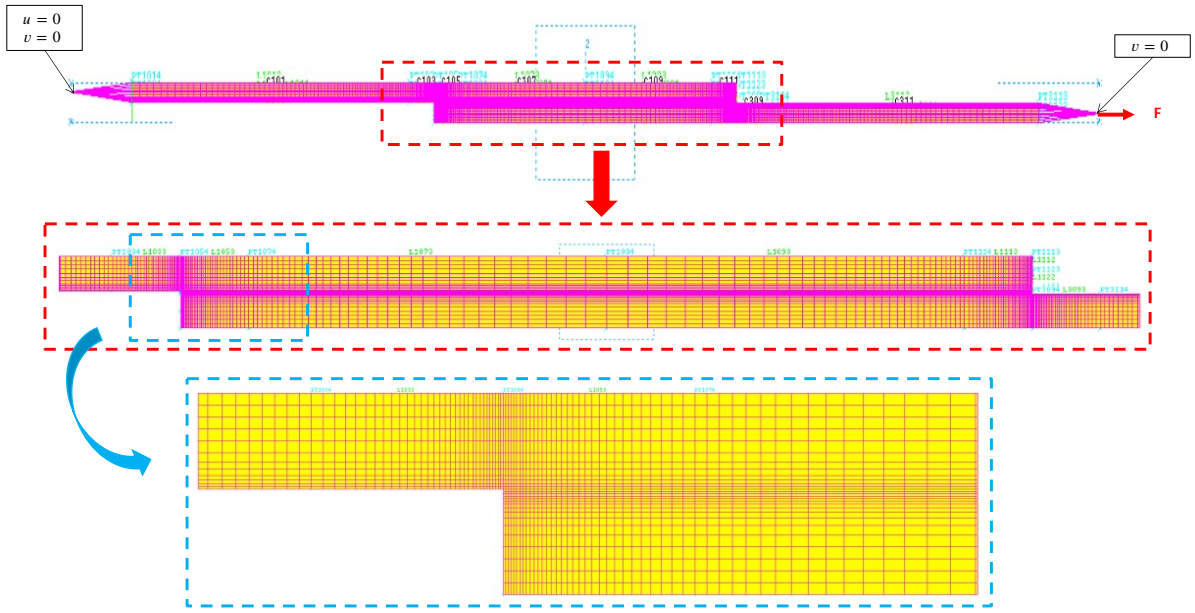

Figure 3: Mesh distribution with aspect/transition ratio in $x = 0$ and in $x = L$ both equal to 1 for a SLJ geometry under the SAMCEF/SIEMENS software

a (mm)	b (mm)	c (mm)	d (mm)	e (mm)	f (mm)	g (mm)	h (mm)
46	4	4	21	21	4	4	46

i (mm)	j (mm)	k (mm)	l (mm)	m (mm)	n (mm)
1	1	0.1	0.1	1	1

Table 1: FEM - Geometric parameters

l_1 (mm)	l_2 (mm)	L (mm)	h_1 (mm)	h_2 (mm)	h_a (mm)	b (mm)
50	50	25	1	1	0.25	25

Table 2: FEM - Geometric parameters

E_1 (MPa)	E_2 (MPa)	E_a (MPa)	ν_1	ν_2	ν_a
70000	70000	2500	0.35	0.35	0.4

Table 3: FEM - Material properties

shear (σ_{xy}) adhesive stresses distributions provided by both models have good agreements. On these stresses in the mid-plane, there is a relative difference of respectively 15.7%, 3.33% and 23.8% on the maximum stresses in the mid-line of the adhesive layer. It can be observed

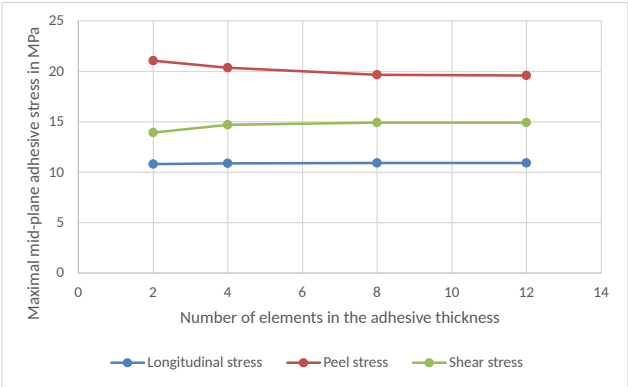

Figure 4: Convergence analysis of the SLJ mesh

the presence of a negative stress peak and values are significantly higher for the presented model. The longitudinal, peel and shear stresses at the free overlap end are negative with the presented model while it tends to zero for the longitudinal stress and remains positive for the peel and the shear stress with the FE model. Thus, on all stresses, an edge effect is present.
To summarize, the presented ME model is an acceptable approximation of the FE model. The three maximal adhesive stresses along the mid-plane are underestimated. On the interfaces, the ME model provides finite stresses values at $x = 0$ and at $x = L$, as well as high stress gradients. The longitudinal stress on the free adhesive edges tends to zero on the FE model while a high peak of negative stress is observable on the presented model. The assumption on the displacement field through the thickness could be the reason by being not enough enriched.

3.3. Recent paper models

3.3.1. Nguyen and Le Grognec model

In their paper [1], the adhesive layer is modeled as a 2D continuous solid satisfying the plane stress hypothesis. The displacement field of the adhesive is identical to the present model (see Eq. 12). The reduced modulus $\lambda_a^{'} = \frac{2\lambda_a}{\lambda+2\mu_a}$ and μ_a are used. The Lamé constant can be expressed in terms of E_a and ν_a with the relation $\lambda_a = \frac{E_a\nu_a}{(1+\nu_a)(1-2\nu_a)}$ and $\mu_a = \frac{E_a}{2(1+\nu_a)}$. From Eq. 7 and [1], the following expression can be extracted:

$$\begin{cases} \sigma_{a,xx} = E_a^{'}\varepsilon_{a,xx} + E_a^{'}\nu_a^{'}\varepsilon_{a,yy} \\ \sigma_{a,xx} = \left(\lambda_a^{'} + 2\mu_a\right)\varepsilon_{a,xx} + \lambda_a^{'}\varepsilon_{a,yy} \end{cases} \tag{32}$$

Therefore, considering the notation used in this paper, Eq. 32 is equivalent to:

$$\begin{cases} E_a^{'} = \dfrac{E_a}{1-\nu_a^2} \\ G_a^{'} = G_a = \dfrac{E_a}{2(1+\nu_a)} \\ \nu_a^{'} = \nu_a \end{cases} \tag{33}$$

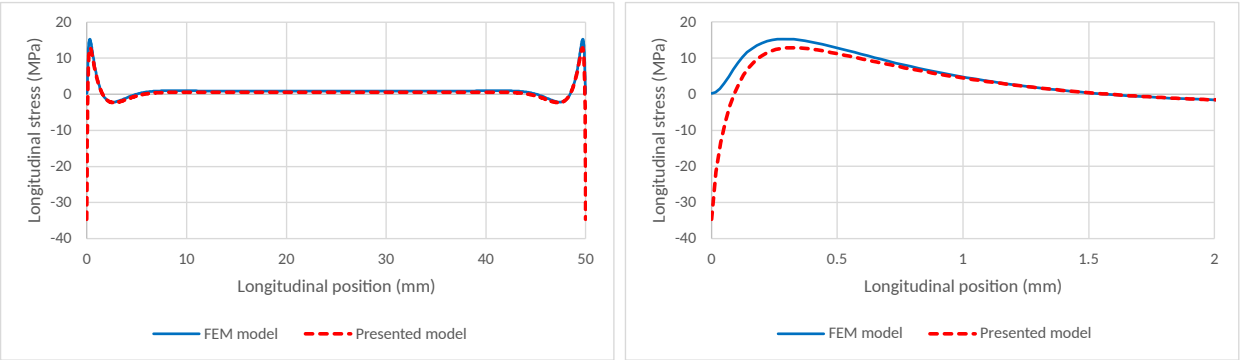

(a) Longitudinal stresses

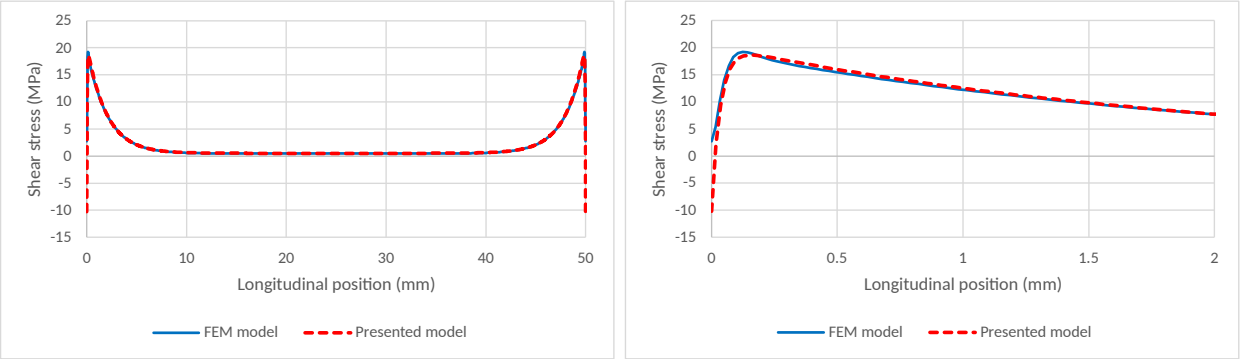

(b) Shear stresses

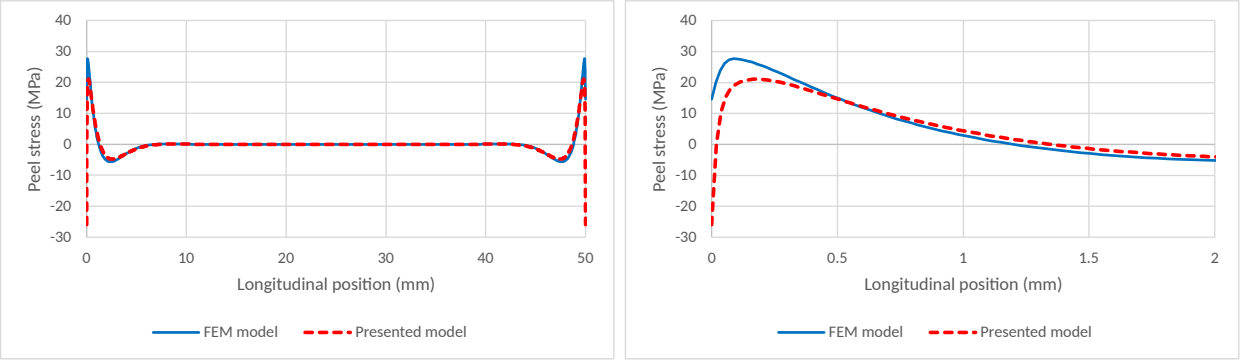

(c) Peel stresses

Figure 5: Comparison between the presented model and the finite element model stresses along the mid-line (i.e. $y = 0$) of the adhesive layer along the overlap (left) and a zoom on the first 2mm (right)

For the upper and lower adherends, Nguyen and Le Grognec [1] considers Timoshenko beams with a shear correction factor k. The Young's modulus E_i, the shear modulus G_i, and the Poisson coefficient ν_i, of the adherend i with $i \in [1, 2]$, are used in such way that:

$$\begin{cases} E_i^{'} = E_i \\ G_i^{'} = kG_i \quad \text{with} \quad G_i = \dfrac{E_i}{2(1+\nu_i)} \quad \text{and} \quad k = \dfrac{5}{6} \\ \nu_i^{'} = 0 \end{cases} \tag{34}$$

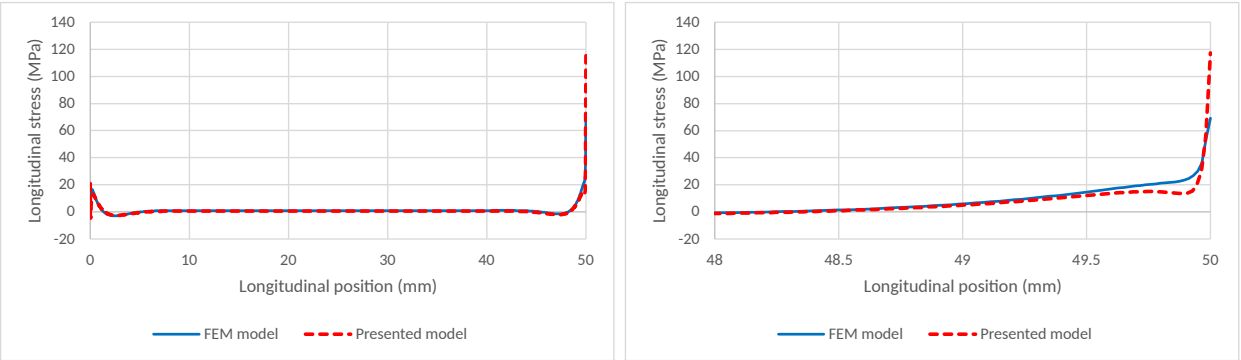

(a) Longitudinal stresses

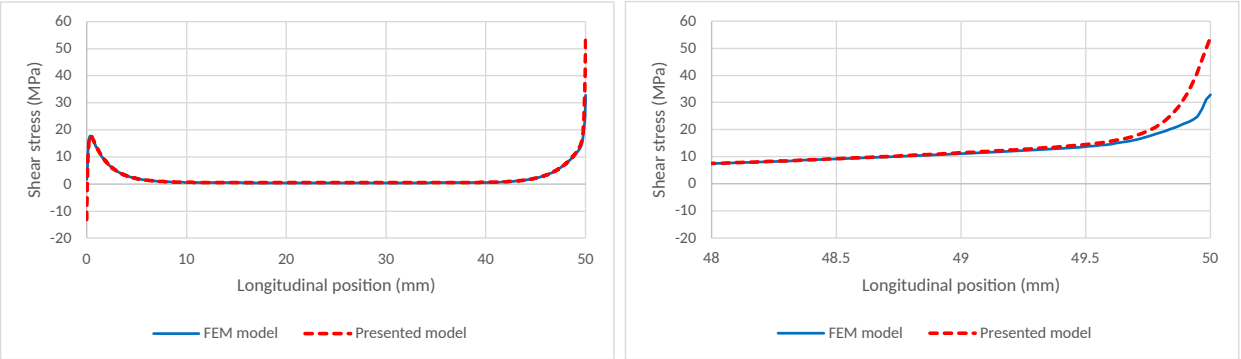

(b) Shear stresses

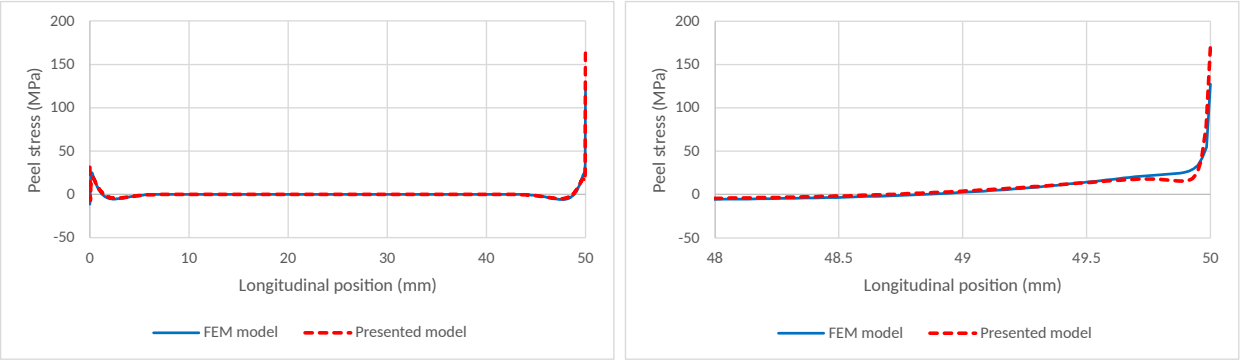

(c) Peel stresses

Figure 6: Comparison between the presented model and the finite element model stresses along the lower interface (i.e. $y = -h_a$) of the adhesive layer along the overlap (left) and a zoom on the last 2mm (right)

The geometric and material parameters considered are respectfully detailed in Table 4 and Table 5. A load F of 5000 N is applied. In Figure 7 and Figure 8, the longitudinal (σ_{xx}),

l_1 (mm)	l_2 (mm)	L (mm)	h_1 (mm)	h_2 (mm)	h_a (mm)	b (mm)
75	75	25	1	1	0.2	25

Table 4: Nguyen and Le Grognec model [1] - Geometric parameters

transverse/peel (σ_{yy}), and shear (σ_{xy}) adhesive stresses are plotted along the overlap length

E_1 (MPa)	E_2 (MPa)	E_a (MPa)	ν_1	ν_2	ν_a
210000	210000	6500	0.3	0.3	0.36

Table 5: Nguyen and Le Grognec model [1] - Material properties

at the mid-line (i.e. $y = 0$) and at the interface (i.e. $y = -h_a$) of the adhesive layer. The longitudinal, shear and peel stress distributions provided by both models are in close agreement. On these stresses, there is a relative difference of respectively 10.5%, 12.4% and 4.60% on the maximum stresses in the mid-line of the adhesive layer, and respectively 68.4%, 27.3% and 68.3% in the upper interface (i.e. $y = +h_a$). The noticeable difference appears on the adhesive edges (i.e. at $x = 0$ and $x = L$). Both models provides longitudinal stress having tendencies to drop to zero at free overlap end (i.e. $x = 0$ and $x = L$). In the same way as in Section 3.2, for both models, it can be observed the presence of a negative stress peak and values are significantly higher for the presented model. The shear stress at the free overlap end remains positive with the model of Nguyen and Le Grognec while it is negative with the presented model.
To summarize, the presented model is able to have close agreement with the Nguyen and Le Grognec model. The same displacement field, for the adherends and the adhesive, is used for both approaches. The difference relies on the resolution scheme. In [1], numerical integrations using Gaussian points are employed for the calculation whereas in the presented approach, an analytical solution is established.

3.3.2. Methfessel and Becker model

In their paper [2], the adhesive layer is modeled as a continuum media, using a special polynomial approaches of higher order and by considering the Ojalvo and Eidinoff [7] displacement approach. The displacement field of the adhesive has a different shape compared to the presented model. It is mainly composed of the adherends displacement and polynomial functions through the adhesive thickness multiplied with unknown adhesive deformation functions. The polynomial functions have been set to vanish at the interface adherend-adhesive. From the three dimensional isotropic Hooke's law and considering the plane strain assumption, the constitutive equations are derived as:

$$\begin{cases} \sigma_{xx}^{(a)} = E^{(a)*}\left(1-\nu^{(a)}\right)\varepsilon_{xx} + E^{(a)*}\nu^{(a)}\varepsilon_{zz} \quad \text{with} \quad E^{(a)*} = \dfrac{E^{(a)}}{\left(1+\nu^{(a)}\right)\left(1-2\nu^{(a)}\right)} \\ \sigma_{a,xx} = E_a^{'}\varepsilon_{a,xx} + E_a^{'}\nu_a^{'}\varepsilon_{a,yy} \end{cases} \tag{35}$$

Considering the notation used in this paper, the following parameters need to be set as:

$$\begin{cases} E_a^{'} = \dfrac{E_a\left(1-\nu_a\right)}{\left(1+\nu_a\right)\left(1-2\nu_a\right)} \\ G_a^{'} = G_a = \dfrac{E_a}{2(1+\nu_a)} \\ \nu_a^{'} = \dfrac{\nu_a}{1-\nu_a} \end{cases} \tag{36}$$

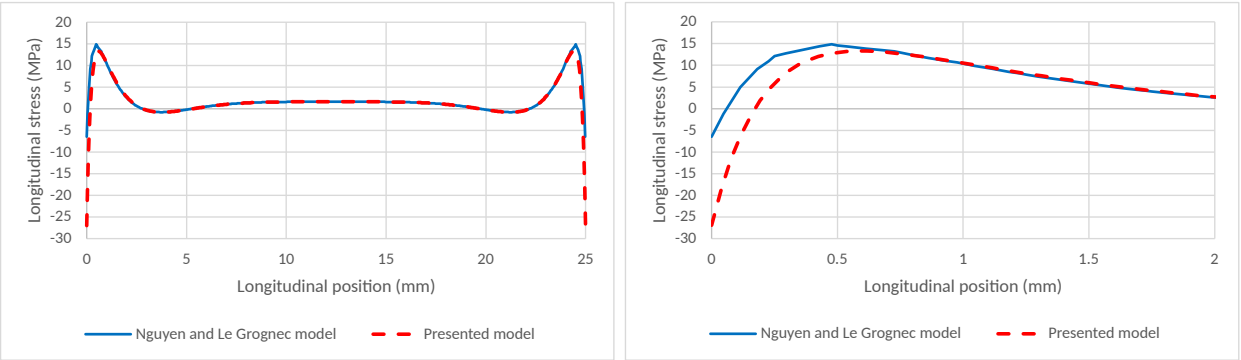

(a) Longitudinal stresses

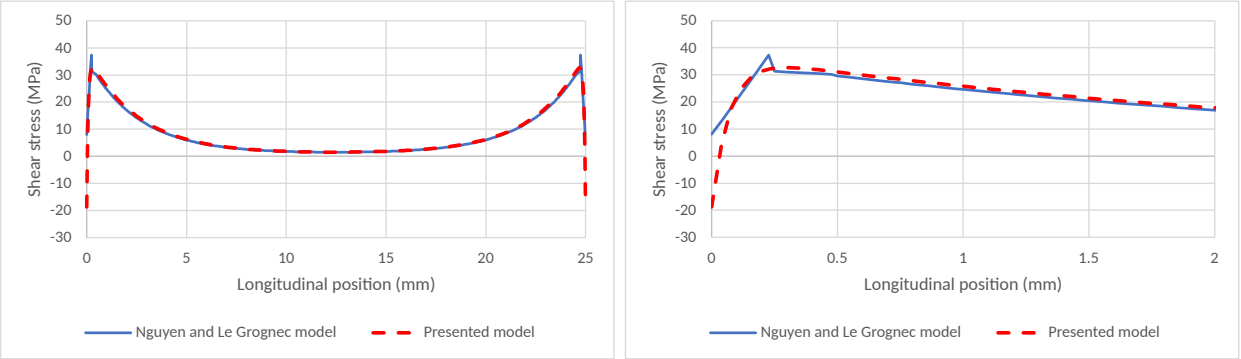

(b) Shear stresses

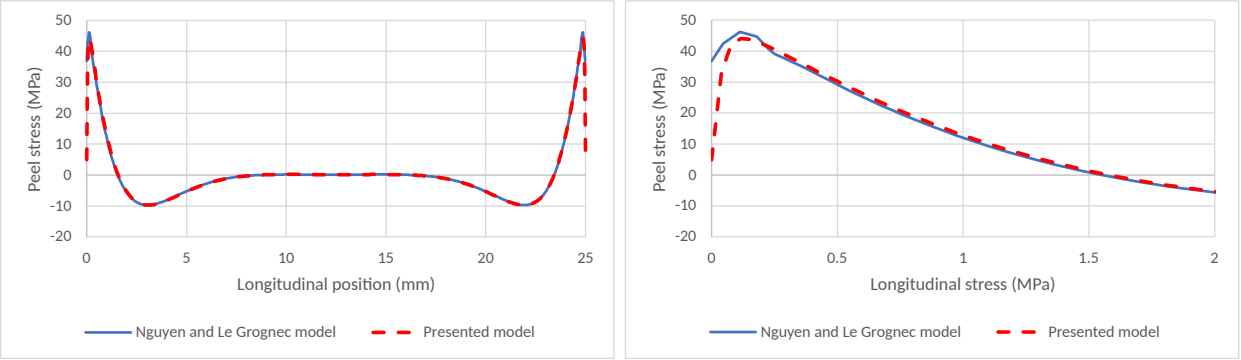

(c) Peel stresses

Figure 7: Comparison between the presented model and the Nguyen and Le Grognec model [1] stresses along the mid-line (i.e. $y = 0$) of the adhesive layer along the overlap

For the upper and lower adherends, Timoshenko beams with a shear correction factor k are considered in [2]. The Young's modulus E_i, the shear modulus G_i, and the Poisson coefficient ν_i, of the adherend i with $i \in [1, 2]$, are the same than Eq. 34.
The geometric and material parameters considered are respectfully detailed in Table 6 and Table 7. A load F of 5000 N is applied. In Figure 9, the longitudinal (σ_{xx}), transverse/peel (σ_{yy}), and shear (σ_{xy}) stresses along the mid-line (i.e. $y = 0$) of the adhesive layer are displayed. In general, good agreements are noticeable. It can be observed the ME model tends to overestimate the maximum shear stress of 19.8% whereas the longitudinal and the peel stresses are well fitted with a relative difference of 0.452% and 1.92% respectively. It

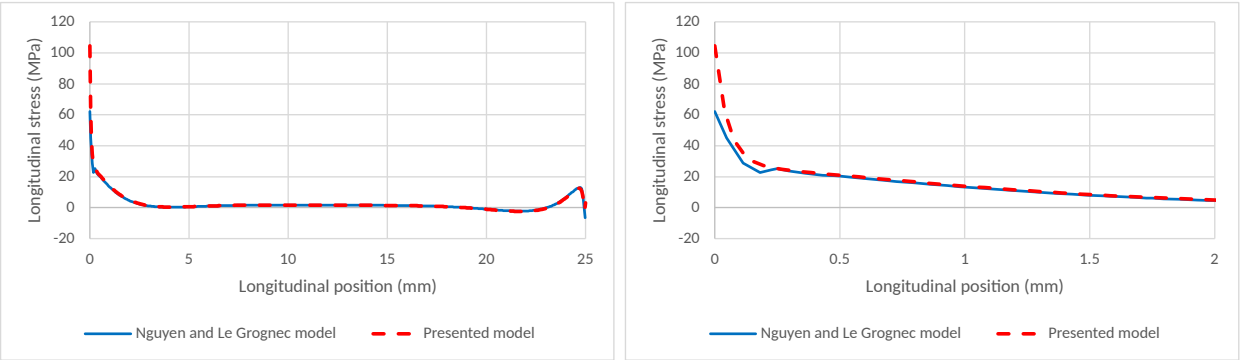

(a) Longitudinal stresses

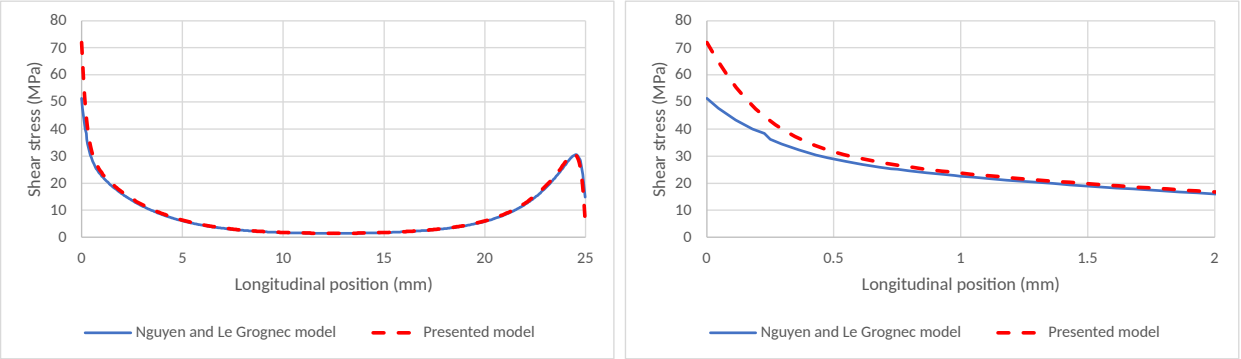

(b) Shear stresses

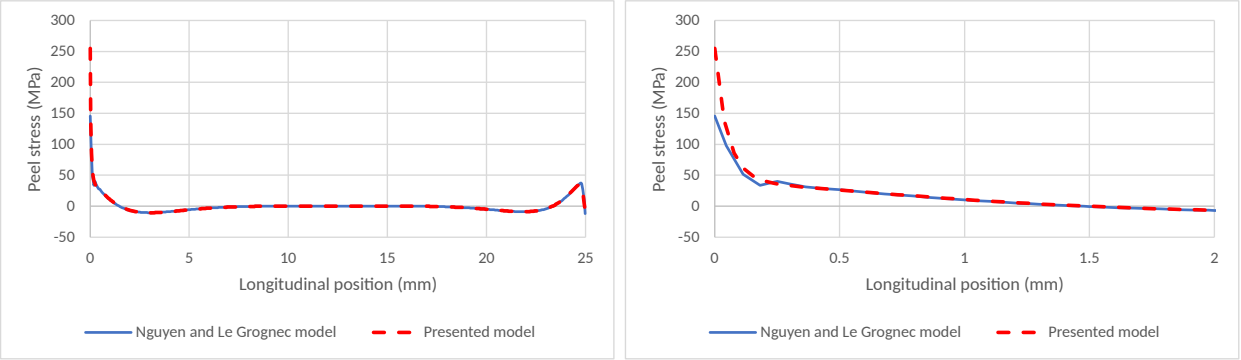

(c) Peel stresses

Figure 8: Comparison between the presented model and the Nguyen and Le Grognec model [1] stresses along the upper interface (i.e. $y = +h_a$) of the adhesive layer along the overlap

l_1 (mm)	l_2 (mm)	L (mm)	h_1 (mm)	h_2 (mm)	h_a (mm)	b (mm)
50	50	25	1	1	0.25	25

Table 6: Methfessel and Becker model [2] - Geometric parameters

should be noted Methfessel and Becker show in [2] that their model underestimates the shear stress compared to those coming from a FE model. A possible justification to this stresses underestimation is the formulation of the displacement field and the stress singularity due

E_1 (MPa)	E_2 (MPa)	E_a (MPa)	ν_1	ν_2	ν_a
210000	210000	2460	0.33	0.33	0.4

Table 7: Methfessel and Becker mode [2] - Material properties

to the geometry, the bi-material interface and boundary conditions. In the same way as in Section 3.3.1, it can be observed the presence of a negative stress peak and values are significantly higher for the presented model. The peel stress at the free overlap end remains positive with the model of Nguyen and Becker while it is negative with the presented model. To summarize, the presented model is able to provide similar results to the Methfessel and Becker model. The displacement field for the adherends is the same for both approaches while for the adhesive it is not. The polynomial degree along the y-coordinate through the adhesive thickness is the same but the adhesive displacement field is expressed in terms of the adherends displacement. The approach for the resolution of ODEs uses as well the matrix exponential but without the stiffness matrix generation such as in this paper.

4. Discussion and conclusion

In this paper, a methodology for the formulation of the stiffness matrix of enriched elements, called continuum macro-element, is presented. The adherends and adhesive are seen as 2D plane continuum media under plane stress or plane strain. The formulation allows for the representation in only one element the full length of a beam. Similarly, when applied to a bonded overlap, the continuum macro-element is modelling in only one element both the adherends and the adhesive all along the overlap length. The resulting SLJ modelling has 24 degree of freedom (DoF). Using only DME as in [21], the structure has 18 DoF but the description of the stress distribution through the thickness is not possible. The DME modelling hypotheses lead to a constant stress distribution along the y-axis in the bounded part. In comparison with the FE model which has 338 333 DoF, the advantage of the CME modelling is clearly visible. It leads to an impressive reduction of computer cost, as highlighted in [32].
The current formulation allows to switch between plane-stress and plane-strain hypotheses. The material parameters used for the formulation allows to cover Timoshenko kinematics, as well as various formulations in the literature, such as [1]. A comparison with finite elements shows acceptable agreement. The proposed model tend to underestimate the longitudinal, shear and peel stresses in the mid-line of the adhesive. A solution to address this phenomena could be the increasing interpolation degree along the y-coordinate (i.e. through the adhesive thickness): it is regarded by the authors as a future work. Moreover, a comparison against two recent models, Nguyen and Le Grognec model [1] and Methfessel and Becker model [2], have shown a good agreement, even if both models use different modelling hypotheses. Some adaptations to the presented model was possible and have been performed to be in line with material properties and to take into consideration the use of Timoshenko beams (see Section 3.3.1 and Section 3.3.2). Beside that, differences still occur. The Nguyen and Le Grognec model [1] needs to mesh the simplified structure with several elements and to use Gaussian quadrature in order to have numerical integrations along both x and y axes. The Methfessel

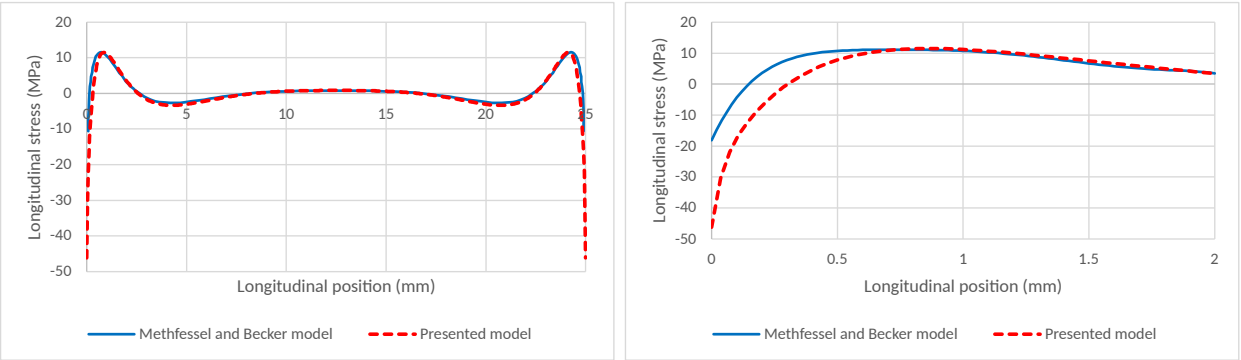

(a) Longitudinal stresses

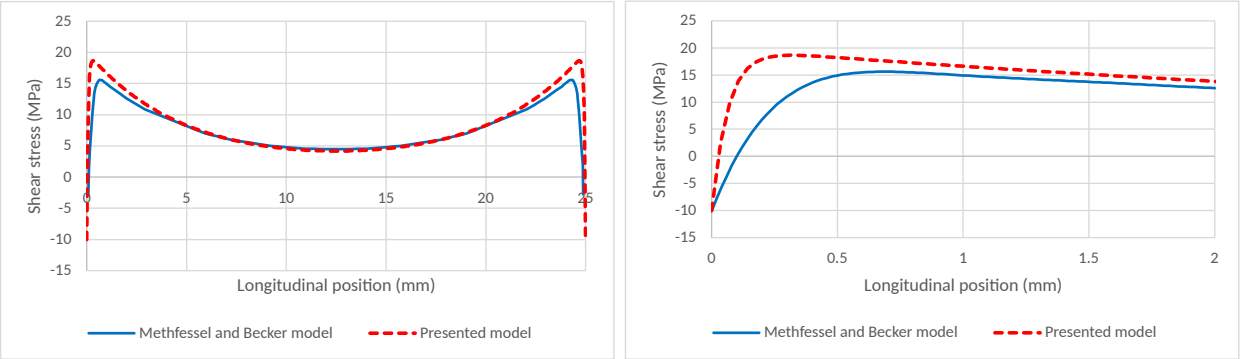

(b) Shear stresses

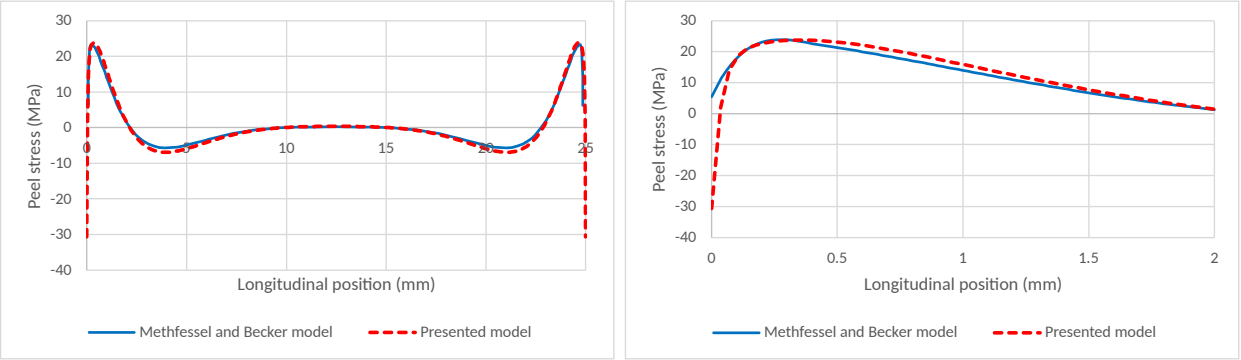

(c) Peel stresses

Figure 9: Comparison between the presented model and the Methfessel and Becker model [2] stresses along the mid-line (i.e. $y = 0$) of the adhesive layer along the overlap (left) and a zoom on the first 2mm (right)

and Becker model [2] use a displacement field along x-axis considering the Ojalvo and Eidinoff displacement approach [7]. The proposed model, available on Github, is able to produce close agreements to those two recent models, with no need of meshing. The SLJ geometry is represented by only 3 elements (see Figure 1), where as the FE modelling needs way more. In addition, the displacement field result in the solution of the sets of ODEs using an analytical approach, allowing the generation of stiffness matrices, in contrast with the FE theory which rely on the supposition of the shape function. As previously demonstrated with the DMEs [23], the ME modelling takes benefits from the existing knowledge on the FE method. Once the elementary stiffness matrices is established, it allows for a simple introduction of various

boundary conditions and loadings, geometrical configurations or material behaviors. This type of modelling wants to be an alternative solution to FE modelling in term of computer efficiency, but using all advantage from FE theory. Its flexibility allows anyone to implement the approach in any language such as Python, or directly inside an existing FE software.
The presented approach presents some limitation. As highlighted in the introduction section, a non-linear geometry behaviour and non-linear material behaviours are not addressed for the presented model. The introduction of the models dedicated to crack onset and propagation could be considered in further steps, following the FE method. Indeed, it was already done with discrete macro-element modelling (see [32]). The free overlap stress is not reached and non-linear geometric behaviour is not possible in the current state. These limitations can be addressed as future work. In general, the use of non-linearity will allow to model complex real life cases.
In a near future, the presented formulation would allow the formulation of an extended version of the CME with the use of a n-order displacement field for the adherend and the adhesive. An improvement of a functionally graded SLJ along the x-axis [33] could be done by adding the y-axis. Based on [29], it would be possible to formulate a multi-layer macroelement, which can be used for the geometry analysis of composite-based material. Finally, as an ultimate improvement, it could be able to address 2D or 3D FE modelling with the use of the presented ME technique.

Conflict of interest

Sébastien Schwartz, Éric Paroissien, Frédéric Lachaud declare that they have no conflict of interest.

Acknowledgements

The authors would like to acknowledge Pr. Le Grognec for providing an Excel sheet with results from [1], which was useful to improve the results and comparisons quality.

Marc Sartor (1957-2022) conceived the first macro-element of adhesively bonded overlap. He offered the opportunity to Éric Paroissien to work on it, without thinking at this time that so many engineering students, doctoral students and professors would have continued the investigations. Éric Paroissien wishes to dedicate this paper to Marc Sartor, an exceptional and humble professor, empathically devoted to the scientific training of his lucky students. In memoriam.

Appendix A. Details

Appendix A.1. Nodal force and displacement vector

For the Timoshenko beam (i.e. adherends without the adhesive), the following formulas is used:

$$U = \begin{bmatrix} u_i(0) \\ u_i(L) \\ v_i(0) \\ v_i(L) \\ \theta_i(0) \\ \theta_i(L) \end{bmatrix} = D.C \quad \text{and} \quad F = \begin{bmatrix} -N_{i,xx}(0) \\ N_{i,xx}(L) \\ -N_{i,xy}(0) \\ N_{i,xy}(L) \\ -M_{i,zz,1}(0) \\ M_{i,zz,1}(L) \end{bmatrix} = L.C \tag{A.1}$$

D and L are squared 6×6 matrix.

For the bonded part (i.e. CME), the following formulas are used:

$$U = \begin{bmatrix} u_1(0) \\ u_0^a(0) \\ u_2(0) \\ u_1(L) \\ u_0^a(L) \\ u_2(L) \\ v_1(0) \\ v_0^a(0) \\ v_2(0) \\ v_1(L) \\ v_0^a(L) \\ v_2(L) \\ \theta_1(0) \\ v_1^a(0) \\ \theta_2(0) \\ \theta_1(L) \\ v_1^a(L) \\ \theta_2(L) \end{bmatrix} = D.C \quad \text{and} \quad F = \begin{bmatrix} -N_{1,xx}(0) \\ -N_{a,xx}(0) \\ -N_{2,xx}(0) \\ N_{1,xx}(L) \\ N_{a,xx}(L) \\ N_{2,xx}(L) \\ -N_{1,xy}(0) \\ -N_{a,xy}(0) \\ -N_{2,xy}(0) \\ N_{1,xy}(L) \\ N_{a,xy}(L) \\ N_{2,xy}(L) \\ -M_{1,zz,1}(0) \\ -M_{a,xy,1}(0) \\ -N_{2,zz,1}(0) \\ M_{1,zz,1}(L) \\ M_{a,xy,1}(L) \\ M_{2,zz,1}(L) \end{bmatrix} = L.C \tag{A.2}$$

D and L are squared 18×18 matrix.

Appendix A.2. Matrix representation

The matrix form of the set of ODEs for the Timoshenko kinematics (i.e. adherends without the adhesive):

$$A = \begin{bmatrix} 0 & 0 & 0 & 1 & 0 & 0 \\ 0 & 0 & 0 & 0 & 1 & 0 \\ 0 & 0 & 0 & 0 & 0 & 1 \\ 0 & 0 & 0 & 0 & 0 & 0 \\ 0 & \frac{3G_i'}{h^2 E_i'} & 0 & 0 & 0 & \frac{3G_i'}{h^2 E_i'} \\ 0 & 0 & 0 & 0 & -1 & 0 \end{bmatrix} \tag{A.3}$$

The matrix form of the set of ODEs for the CME:

$$
A = \begin{bmatrix}
0 & 0 & 0 & 0 & 0 & 0 & 0 & 0 & 0 & 1 & 0 & 0 & 0 & 0 & 0 & 0 & 0 & 0 \\
0 & 0 & 0 & 0 & 0 & 0 & 0 & 0 & 0 & 0 & 1 & 0 & 0 & 0 & 0 & 0 & 0 & 0 \\
0 & 0 & 0 & 0 & 0 & 0 & 0 & 0 & 0 & 0 & 0 & 1 & 0 & 0 & 0 & 0 & 0 & 0 \\
0 & 0 & 0 & 0 & 0 & 0 & 0 & 0 & 0 & 0 & 0 & 0 & 1 & 0 & 0 & 0 & 0 & 0 \\
0 & 0 & 0 & 0 & 0 & 0 & 0 & 0 & 0 & 0 & 0 & 0 & 0 & 1 & 0 & 0 & 0 & 0 \\
0 & 0 & 0 & 0 & 0 & 0 & 0 & 0 & 0 & 0 & 0 & 0 & 0 & 0 & 1 & 0 & 0 & 0 \\
0 & 0 & 0 & 0 & 0 & 0 & 0 & 0 & 0 & 0 & 0 & 0 & 0 & 0 & 0 & 1 & 0 & 0 \\
0 & 0 & 0 & 0 & 0 & 0 & 0 & 0 & 0 & 0 & 0 & 0 & 0 & 0 & 0 & 0 & 1 & 0 \\
0 & 0 & 0 & 0 & 0 & 0 & 0 & 0 & 0 & 0 & 0 & 0 & 0 & 0 & 0 & 0 & 0 & 1 \\
\frac{a_{11}}{a_{10}} & \frac{a_{12}}{a_{10}} & \frac{a_{13}}{a_{10}} & \frac{a_{14}}{a_{10}} & \frac{a_{15}}{a_{10}} & 0 & 0 & 0 & 0 & 0 & 0 & 0 & 0 & 0 & \frac{a_{16}}{a_{10}} & \frac{a_{17}}{a_{10}} & \frac{a_{18}}{a_{10}} & \frac{a_{19}}{a_{10}} \\
\frac{a_{21}}{a_{20}} & \frac{a_{22}}{a_{20}} & \frac{a_{23}}{a_{20}} & \frac{a_{24}}{a_{20}} & \frac{a_{25}}{a_{20}} & 0 & 0 & 0 & 0 & 0 & 0 & 0 & 0 & 0 & \frac{a_{26}}{a_{20}} & \frac{a_{27}}{a_{20}} & \frac{a_{28}}{a_{20}} & \frac{a_{29}}{a_{20}} \\
\frac{a_{31}}{a_{30}} & \frac{a_{32}}{a_{30}} & \frac{a_{33}}{a_{30}} & \frac{a_{34}}{a_{30}} & \frac{a_{35}}{a_{30}} & 0 & 0 & 0 & 0 & 0 & 0 & 0 & 0 & 0 & \frac{a_{36}}{a_{30}} & \frac{a_{37}}{a_{30}} & \frac{a_{38}}{a_{30}} & \frac{a_{39}}{a_{30}} \\
\frac{a_{41}}{a_{40}} & \frac{a_{42}}{a_{40}} & \frac{a_{43}}{a_{40}} & \frac{a_{44}}{a_{40}} & \frac{a_{45}}{a_{40}} & 0 & 0 & 0 & 0 & 0 & 0 & 0 & 0 & 0 & \frac{a_{46}}{a_{40}} & \frac{a_{47}}{a_{40}} & \frac{a_{48}}{a_{40}} & \frac{a_{49}}{a_{40}} \\
\frac{a_{51}}{a_{50}} & \frac{a_{52}}{a_{50}} & \frac{a_{53}}{a_{50}} & \frac{a_{54}}{a_{50}} & \frac{a_{55}}{a_{50}} & 0 & 0 & 0 & 0 & 0 & 0 & 0 & 0 & 0 & \frac{a_{56}}{a_{50}} & \frac{a_{57}}{a_{50}} & \frac{a_{58}}{a_{50}} & \frac{a_{59}}{a_{50}} \\
0 & 0 & 0 & 0 & 0 & \frac{a_{61}}{a_{60}} & \frac{a_{62}}{a_{60}} & \frac{a_{63}}{a_{60}} & \frac{a_{64}}{a_{60}} & \frac{a_{65}}{a_{60}} & \frac{a_{66}}{a_{60}} & \frac{a_{67}}{a_{60}} & \frac{a_{68}}{a_{60}} & \frac{a_{69}}{a_{60}} & 0 & 0 & 0 & 0 \\
0 & 0 & 0 & 0 & 0 & \frac{a_{71}}{a_{70}} & \frac{a_{72}}{a_{70}} & \frac{a_{73}}{a_{70}} & \frac{a_{74}}{a_{70}} & \frac{a_{75}}{a_{70}} & \frac{a_{76}}{a_{70}} & \frac{a_{77}}{a_{70}} & \frac{a_{78}}{a_{70}} & \frac{a_{79}}{a_{70}} & 0 & 0 & 0 & 0 \\
0 & 0 & 0 & 0 & 0 & \frac{a_{81}}{a_{80}} & \frac{a_{82}}{a_{80}} & \frac{a_{83}}{a_{80}} & \frac{a_{84}}{a_{80}} & \frac{a_{85}}{a_{80}} & \frac{a_{86}}{a_{80}} & \frac{a_{87}}{a_{80}} & \frac{a_{88}}{a_{80}} & \frac{a_{89}}{a_{80}} & 0 & 0 & 0 & 0 \\
0 & 0 & 0 & 0 & 0 & \frac{a_{91}}{a_{90}} & \frac{a_{92}}{a_{90}} & \frac{a_{93}}{a_{90}} & \frac{a_{94}}{a_{90}} & \frac{a_{95}}{a_{90}} & \frac{a_{96}}{a_{90}} & \frac{a_{97}}{a_{90}} & \frac{a_{98}}{a_{90}} & \frac{a_{99}}{a_{90}} & 0 & 0 & 0 & 0
\end{bmatrix} \tag{A.4}
$$

$$
\begin{aligned}
a_{10} &= h_a^2 E_a^{'}\left(18E_1^{'}E_2^{'}h_1h_2+9E_1^{'}E_a^{'}h_1h_a+9E_2^{'}E_a^{'}h_2h_a+4E_a^{'2}h_a^2\right)\\
a_{11} &= -\frac{1}{4}\left(-180E_1^{'}E_2^{'}G_a^{'}h_1h_2-120E_1^{'}E_a^{'}G_a^{'}h_1h_a-120E_2^{'}E_a^{'}G_a^{'}h_2h_a-80E_a^{'2}G_a^{'}h_a^2\right)\\
a_{12} &= -\frac{1}{4}\left(90E_1^{'}E_2^{'}G_a^{'}h_1h_2+51E_1^{'}E_a^{'}G_a^{'}h_1h_a+69E_2^{'}E_a^{'}G_a^{'}h_2h_a+40E_a^{'2}G_a^{'}h_a^2\right)\\
a_{13} &= -\frac{1}{4}\Big(-90E_1^{'}E_2^{'}G_a^{'}h_1^2h_2-51E_1^{'}E_a^{'}G_a^{'}h_1^2h_a-27E_2^{'}E_a^{'}G_1^{'}h_2h_a^2\\
&\quad -69E_2^{'}E_a^{'}G_a^{'}h_1h_2h_a-18E_a^{'2}G_1^{'}h_a^3-40E_a^{'2}G_a^{'}h_1h_a^2\Big)\\
a_{14} &= -\frac{1}{4}\left(90E_1^{'}E_2^{'}G_a^{'}h_1h_2+69E_1^{'}E_a^{'}G_a^{'}h_1h_a+51E_2^{'}E_a^{'}G_a^{'}h_2h_a+40E_a^{'2}G_a^{'}h_a^2\right)\\
a_{15} &= -\frac{1}{4}\Big(90E_1^{'}E_2^{'}G_a^{'}h_1h_2^2+27E_1^{'}E_a^{'}G_2^{'}h_1h_a^2+69E_1^{'}E_a^{'}G_a^{'}h_1h_2h_a+51E_2^{'}E_a^{'}G_a^{'}h_2^2h_a\\
&\quad +18E_a^{'2}G_2^{'}h_a^3+40E_a^{'2}G_a^{'}h_2h_a^2\Big)\\
a_{16} &= -\frac{1}{4}\Big(-12E_1^{'}E_a^{'2}h_1h_a^2\nu_a^{'}+12E_2^{'}E_a^{'2}h_2h_a^2\nu_a^{'}-12E_1^{'}E_a^{'}G_a^{'}h_1h_a^2\\
&\quad +12E_2^{'}E_a^{'}G_a^{'}h_2h_a^2\Big)\\
a_{17} &= -\frac{1}{4}\Big(36E_1^{'}E_2^{'}E_a^{'}h_1h_2h_a^2\nu_a^{'}+24E_1^{'}E_a^{'2}h_1h_a^3\nu_a^{'}+24E_2^{'}E_a^{'2}h_2h_a^3\nu_a^{'}\\
&\quad +16E_a^{'3}h_a^4\nu_a^{'}+36E_1^{'}E_2^{'}G_a^{'}h_1h_2h_a^2+24E_1^{'}E_a^{'}G_a^{'}h_1h_a^3\\
&\quad +24E_2^{'}E_a^{'}G_a^{'}h_2h_a^3+16E_a^{'2}G_a^{'}h_a^4\Big)\\
a_{18} &= -\frac{1}{4}\Big(27E_1^{'}E_2^{'}E_a^{'}h_1h_2h_a\nu_a^{'}+15E_1^{'}E_a^{'2}h_1h_a^2\nu_a^{'}+3E_2^{'}E_a^{'2}h_2h_a^2\nu_a^{'}\\
&\quad +27E_1^{'}E_2^{'}G_a^{'}h_1h_2h_a+15E_1^{'}E_a^{'}G_a^{'}h_1h_a^2-27E_2^{'}E_a^{'}G_1^{'}h_2h_a^2+21E_2^{'}E_a^{'}G_a^{'}h_2h_a^2\\
&\quad -18E_a^{'2}G_1^{'}h_a^3+12E_a^{'2}G_a^{'}h_a^3\Big)\\
a_{19} &= -\frac{1}{4}\Big(-27E_1^{'}E_2^{'}E_a^{'}h_1h_2h_a\nu_a^{'}-3E_1^{'}E_a^{'2}h_1h_a^2\nu_a^{'}-15E_2^{'}E_a^{'2}h_2h_a^2\nu_a^{'}\\
&\quad -27E_1^{'}E_2^{'}G_a^{'}h_1h_2h_a+27E_1^{'}E_a^{'}G_2^{'}h_1h_a^2-21E_1^{'}E_a^{'}G_a^{'}h_1h_a^2-15E_2^{'}E_a^{'}G_a^{'}h_2h_a^2\\
&\quad +18E_a^{'2}G_2^{'}h_a^3-12E_a^{'2}G_a^{'}h_a^3\Big)
\end{aligned}
\tag{A.5}
$$

$$
\begin{aligned}
a_{20} &= h_a h_1 E_1^{'}\left(18E_1^{'}E_2^{'}h_1h_2 + 9E_1^{'}E_a^{'}h_1h_a + 9E_2^{'}E_a^{'}h_2h_a + 4E_a^{'2}h_a^2\right)\\
a_{21} &= \frac{1}{4}\left(-60E_1^{'}E_2^{'}G_a^{'}h_1h_2 - 40E_1^{'}E_a^{'}G_a^{'}h_1h_a\right)\\
a_{22} &= \frac{1}{4}\left(48E_1^{'}E_2^{'}G_a^{'}h_1h_2 + 26E_1^{'}E_a^{'}G_a^{'}h_1h_a\right)\\
a_{23} &= \frac{1}{4}\left(-48E_1^{'}E_2^{'}G_a^{'}h_1^2h_2 - 26E_1^{'}E_a^{'}G_a^{'}h_1^2h_a + 27E_2^{'}E_a^{'}G_1^{'}h_2h_a^2 + 12E_a^{'2}G_1^{'}h_a^3\right)\\
a_{24} &= \frac{1}{4}\left(12E_1^{'}E_2^{'}G_a^{'}h_1h_2 + 14E_1^{'}E_a^{'}G_a^{'}h_1h_a\right)\\
a_{25} &= \frac{1}{4}\left(12E_1^{'}E_2^{'}G_a^{'}h_1h_2^2 + 9E_1^{'}E_a^{'}G_2^{'}h_1h_a^2 + 14E_1^{'}E_a^{'}G_a^{'}h_1h_2h_a\right)\\
a_{26} &= \frac{1}{4}\Big(24E_1^{'}E_2^{'}E_a^{'}h_1h_2h_a\nu_a^{'} + 8E_1^{'}E_a^{'2}h_1h_a^2\nu_a^{'} + 24E_1^{'}E_2^{'}G_a^{'}h_1h_2h_a\\
&\quad +8E_1^{'}E_a^{'}G_a^{'}h_1h_a^2\Big)\\
a_{27} &= \frac{1}{4}\Big(12E_1^{'}E_2^{'}E_a^{'}h_1h_2h_a^2\nu_a^{'} + 8E_1^{'}E_a^{'2}h_1h_a^3\nu_a^{'} + 12E_1^{'}E_2^{'}G_a^{'}h_1h_2h_a^2\\
&\quad +8E_1^{'}E_a^{'}G_a^{'}h_1h_a^3\Big)\\
a_{28} &= \frac{1}{4}\Big(-21E_1^{'}E_2^{'}E_a^{'}h_1h_2h_a\nu_a^{'} - 10E_1^{'}E_a^{'2}h_1h_a^2\nu_a^{'} + 15E_1^{'}E_2^{'}G_a^{'}h_1h_2h_a\\
&\quad +8E_1^{'}E_a^{'}G_a^{'}h_1h_a^2 + 27E_2^{'}E_a^{'}G_1^{'}h_2h_a^2 + 12E_a^{'2}G_1^{'}h_a^3\Big)\\
a_{29} &= \frac{1}{4}\Big(-3E_1^{'}E_2^{'}E_a^{'}h_1h_2h_a\nu_a^{'} + 2E_1^{'}E_a^{'2}h_1h_a^2\nu_a^{'} - 3E_1^{'}E_2^{'}G_a^{'}h_1h_2h_a\\
&\quad +9E_1^{'}E_a^{'}G_2^{'}h_1h_a^2 - 4E_1^{'}E_a^{'}G_a^{'}h_1h_a^2\Big)
\end{aligned}
\tag{A.6}
$$

$$
\begin{aligned}
a_{30} &= E_1^{'} h_1^2 h_a \left(18 E_1^{'} E_2^{'} h_1 h_2 + 9 E_1^{'} E_a^{'} h_1 h_a + 9 E_2^{'} E_a^{'} h_2 h_a + 4 E_a^{'2} h_a^2\right) \\
a_{31} &= -\frac{3}{4}\left(-60 E_1^{'} E_2^{'} G_a^{'} h_1 h_2 - 40 E_1^{'} E_a^{'} G_a^{'} h_1 h_a\right) \\
a_{32} &= -\frac{3}{4}\left(48 E_1^{'} E_2^{'} G_a^{'} h_1 h_2 + 26 E_1^{'} E_a^{'} G_a^{'} h_1 h_a\right) \\
a_{33} &= -\frac{3}{4}\Big(-72 E_1^{'} E_2^{'} G_1^{'} h_1 h_2 h_a - 48 E_1^{'} E_2^{'} G_a^{'} h_1^2 h_2 - 36 E_1^{'} E_a^{'} G_1^{'} h_1 h_a^2 \\
&\quad -26 E_1^{'} E_a^{'} G_a^{'} h_1^2 h_a - 9 E_2^{'} E_a^{'} G_1^{'} h_2 h_a^2 - 4 E_a^{'2} G_1^{'} h_a^3\Big) \\
a_{34} &= -\frac{3}{4}\left(12 E_1^{'} E_2^{'} G_a^{'} h_1 h_2 + 14 E_1^{'} E_a^{'} G_a^{'} h_1 h_a\right) \\
a_{35} &= -\frac{3}{4}\left(12 E_1^{'} E_2^{'} G_a^{'} h_1 h_2^2 + 9 E_1^{'} E_a^{'} G_2^{'} h_1 h_a^2 + 14 E_1^{'} E_a^{'} G_a^{'} h_1 h_2 h_a\right) \\
a_{36} &= -\frac{3}{4}\Big(24 E_1^{'} E_2^{'} E_a^{'} h_1 h_2 h_a \nu_a^{'} + 8 E_1^{'} E_a^{'2} h_1 h_a^2 \nu_a^{'} + 24 E_1^{'} E_2^{'} G_a^{'} h_1 h_2 h_a \\
&\quad +8 E_1^{'} E_a^{'} G_a^{'} h_1 h_a^2\Big) \\
a_{37} &= -\frac{3}{4}\Big(12 E_1^{'} E_2^{'} E_a^{'} h_1 h_2 h_a^2 \nu_a^{'} + 8 E_1^{'} E_a^{'2} h_1 h_a^3 \nu_a^{'} + 12 E_1^{'} E_2^{'} G_a^{'} h_1 h_2 h_a^2 \\
&\quad +8 E_1^{'} E_a^{'} G_a^{'} h_1 h_a^3\Big) \\
a_{38} &= -\frac{3}{4}\Big(-21 E_1^{'} E_2^{'} E_a^{'} h_1 h_2 h_a \nu_a^{'} - 10 E_1^{'} E_a^{'2} h_1 h_a^2 \nu_a^{'} - 72 E_1^{'} E_2^{'} G_1^{'} h_1 h_2 h_a \\
&\quad +15 E_1^{'} E_2^{'} G_a^{'} h_1 h_2 h_a - 36 E_1^{'} E_a^{'} G_1^{'} h_1 h_a^2 + 8 E_1^{'} E_a^{'} G_a^{'} h_1 h_a^2 \\
&\quad -9 E_2^{'} E_a^{'} G_1^{'} h_2 h_a^2 - 4 E_a^{'2} G_1^{'} h_a^3\Big) \\
a_{39} &= -\frac{3}{4}\Big(-3 E_1^{'} E_2^{'} E_a^{'} h_1 h_2 h_a \nu_a^{'} + 2 E_1^{'} E_a^{'2} h_1 h_a^2 \nu_a^{'} - 3 E_1^{'} E_2^{'} G_a^{'} h_1 h_2 h_a \\
&\quad +9 E_1^{'} E_a^{'} G_2^{'} h_1 h_a^2 - 4 E_1^{'} E_a^{'} G_a^{'} h_1 h_a^2\Big)
\end{aligned}
\tag{A.7}
$$

$$
\begin{aligned}
a_{40} &= h_2 E_2^{'} h_a \left(18 E_1^{'} E_2^{'} h_1 h_2 + 9 E_1^{'} E_a^{'} h_1 h_a + 9 E_2^{'} E_a^{'} h_2 h_a + 4 E_a^{'2} h_a^2\right) \\
a_{41} &= \frac{1}{4}\left(-60 E_1^{'} E_2^{'} G_a^{'} h_1 h_2 - 40 E_2^{'} E_a^{'} G_a^{'} h_2 h_a\right) \\
a_{42} &= \frac{1}{4}\left(12 E_1^{'} E_2^{'} G_a^{'} h_1 h_2 + 14 E_2^{'} E_a^{'} G_a^{'} h_2 h_a\right) \\
a_{43} &= \frac{1}{4}\left(-12 E_1^{'} E_2^{'} G_a^{'} h_1^2 h_2 - 9 E_2^{'} E_a^{'} G_1^{'} h_2 h_a^2 - 14 E_2^{'} E_a^{'} G_a^{'} h_1 h_2 h_a\right) \\
a_{44} &= \frac{1}{4}\left(48 E_1^{'} E_2^{'} G_a^{'} h_1 h_2 + 26 E_2^{'} E_a^{'} G_a^{'} h_2 h_a\right) \\
a_{45} &= \frac{1}{4}\left(48 E_1^{'} E_2^{'} G_a^{'} h_1 h_2^2 - 27 E_1^{'} E_a^{'} G_2^{'} h_1 h_a^2 + 26 E_2^{'} E_a^{'} G_a^{'} h_2^2 h_a - 12 E_a^{'2} G_2^{'} h_a^3\right) \\
a_{46} &= \frac{1}{4}\Big(-24 E_1^{'} E_2^{'} E_a^{'} h_1 h_2 h_a \nu_a^{'} - 8 E_2^{'} E_a^{'2} h_2 h_a^2 \nu_a^{'} - 24 E_1^{'} E_2^{'} G_a^{'} h_1 h_2 h_a \\
&\quad -8 E_2^{'} E_a^{'} G_a^{'} h_2 h_a^2\Big) \\
a_{47} &= \frac{1}{4}\Big(12 E_1^{'} E_2^{'} E_a^{'} h_1 h_2 h_a^2 \nu_a^{'} + 8 E_2^{'} E_a^{'2} h_2 h_a^3 \nu_a^{'} + 12 E_1^{'} E_2^{'} G_a^{'} h_1 h_2 h_a^2 \\
&\quad +8 E_2^{'} E_a^{'} G_a^{'} h_2 h_a^3\Big) \\
a_{48} &= \frac{1}{4}\Big(3 E_1^{'} E_2^{'} E_a^{'} h_1 h_2 h_a \nu_a^{'} - 2 E_2^{'} E_a^{'2} h_2 h_a^2 \nu_a^{'} + 3 E_1^{'} E_2^{'} G_a^{'} h_1 h_2 h_a \\
&\quad -9 E_2^{'} E_a^{'} G_1^{'} h_2 h_a^2 + 4 E_2^{'} E_a^{'} G_a^{'} h_2 h_a^2\Big) \\
a_{49} &= \frac{1}{4}\Big(21 E_1^{'} E_2^{'} E_a^{'} h_1 h_2 h_a \nu_a^{'} + 10 E_2^{'} E_a^{'2} h_2 h_a^2 \nu_a^{'} - 15 E_1^{'} E_2^{'} G_a^{'} h_1 h_2 h_a \\
&\quad -27 E_1^{'} E_a^{'} G_2^{'} h_1 h_a^2 - 8 E_2^{'} E_a^{'} G_a^{'} h_2 h_a^2 - 12 E_a^{'2} G_2^{'} h_a^3\Big)
\end{aligned}
\tag{A.8}
$$

$$
\begin{aligned}
a_{50} &= E_2^{'} h_2^2 h_a \left(18 E_1^{'} E_2^{'} h_1 h_2 + 9 E_1^{'} E_a^{'} h_1 h_a + 9 E_2^{'} E_a^{'} h_2 h_a + 4 E_a^{'2} h_a^2\right) \\
a_{51} &= \frac{3}{4}\left(-60 E_1^{'} E_2^{'} G_a^{'} h_1 h_2 - 40 E_2^{'} E_a^{'} G_a^{'} h_2 h_a\right) \\
a_{52} &= \frac{3}{4}\left(12 E_1^{'} E_2^{'} G_a^{'} h_1 h_2 + 14 E_2^{'} E_a^{'} G_a^{'} h_2 h_a\right) \\
a_{53} &= \frac{3}{4}\left(-12 E_1^{'} E_2^{'} G_a^{'} h_1^2 h_2 - 9 E_2^{'} E_a^{'} G_1^{'} h_2 h_a^2 - 14 E_2^{'} E_a^{'} G_a^{'} h_1 h_2 h_a\right) \\
a_{54} &= \frac{3}{4}\left(48 E_1^{'} E_2^{'} G_a^{'} h_1 h_2 + 26 E_2^{'} E_a^{'} G_a^{'} h_2 h_a\right) \\
a_{55} &= \frac{3}{4}\Big(72 E_1^{'} E_2^{'} G_2^{'} h_1 h_2 h_a + 48 E_1^{'} E_2^{'} G_a^{'} h_1 h_2^2 + 9 E_1^{'} E_a^{'} G_2^{'} h_1 h_a^2 \\
&\quad + 36 E_2^{'} E_a^{'} G_2^{'} h_2 h_a^2 + 26 E_2^{'} E_a^{'} G_a^{'} h_2^2 h_a + 4 E_a^{'2} G_2^{'} h_a^3\Big) \\
a_{56} &= \frac{3}{4}\Big(-24 E_1^{'} E_2^{'} E_a^{'} h_1 h_2 h_a \nu_a^{'} - 8 E_2^{'} E_a^{'2} h_2 h_a^2 \nu_a^{'} - 24 E_1^{'} E_2^{'} G_a^{'} h_1 h_2 h_a \\
&\quad - 8 E_2^{'} E_a^{'} G_a^{'} h_2 h_a^2\Big) \\
a_{57} &= \frac{3}{4}\Big(12 E_1^{'} E_2^{'} E_a^{'} h_1 h_2 h_a^2 \nu_a^{'} + 8 E_2^{'} E_a^{'2} h_2 h_a^3 \nu_a^{'} + 12 E_1^{'} E_2^{'} G_a^{'} h_1 h_2 h_a^2 \\
&\quad + 8 E_2^{'} E_a^{'} G_a^{'} h_2 h_a^3\Big) \\
a_{58} &= \frac{3}{4}\Big(3 E_1^{'} E_2^{'} E_a^{'} h_1 h_2 h_a \nu_a^{'} - 2 E_2^{'} E_a^{'2} h_2 h_a^2 \nu_a^{'} + 3 E_1^{'} E_2^{'} G_a^{'} h_1 h_2 h_a \\
&\quad - 9 E_2^{'} E_a^{'} G_1^{'} h_2 h_a^2 + 4 E_2^{'} E_a^{'} G_a^{'} h_2 h_a^2\Big) \\
a_{59} &= \frac{3}{4}\Big(21 E_1^{'} E_2^{'} E_a^{'} h_1 h_2 h_a \nu_a^{'} + 10 E_2^{'} E_a^{'2} h_2 h_a^2 \nu_a^{'} + 72 E_1^{'} E_2^{'} G_2^{'} h_1 h_2 h_a \\
&\quad - 15 E_1^{'} E_2^{'} G_a^{'} h_1 h_2 h_a + 9 E_1^{'} E_a^{'} G_2^{'} h_1 h_a^2 + 36 E_2^{'} E_a^{'} G_2^{'} h_2 h_a^2 \\
&\quad - 8 E_2^{'} E_a^{'} G_a^{'} h_2 h_a^2 + 4 E_a^{'2} G_2^{'} h_a^3\Big)
\end{aligned}
\tag{A.9}
$$

$$
\begin{aligned}
a_{60} &= h_a^2 G_a^{'} b \left(240 G_1^{'} G_2^{'} h_1 h_2 + 16 G_1^{'} G_a^{'} h_1 h_a + 16 G_2^{'} G_a^{'} h_2 h_a + G_a^{'2} h_a^2\right) \\
a_{61} &= -\frac{1}{4}\Big(-2400 E_a^{'} G_1^{'} G_2^{'} b h_1 h_2 - 260 E_a^{'} G_1^{'} G_a^{'} b h_1 h_a - 260 E_a^{'} G_2^{'} G_a^{'} b h_2 h_a \\
&\quad -20 E_a^{'} G_a^{'2} b h_a^2\Big) \\
a_{62} &= -\frac{1}{4}\Big(84 E_a^{'} G_1^{'} G_a^{'} b h_1 h_a^2 - 84 E_a^{'} G_2^{'} G_a^{'} b h_2 h_a^2\Big) \\
a_{63} &= -\frac{1}{4}\Big(1200 E_a^{'} G_1^{'} G_2^{'} b h_1 h_2 + 58 E_a^{'} G_1^{'} G_a^{'} b h_1 h_a + 202 E_a^{'} G_2^{'} G_a^{'} b h_2 h_a \\
&\quad +10 E_a^{'} G_a^{'2} b h_a^2\Big) \\
a_{64} &= -\frac{1}{4}\Big(1200 E_a^{'} G_1^{'} G_2^{'} b h_1 h_2 + 202 E_a^{'} G_1^{'} G_a^{'} b h_1 h_a + 58 E_a^{'} G_2^{'} G_a^{'} b h_2 h_a \\
&\quad +10 E_a^{'} G_a^{'2} b h_a^2\Big) \\
a_{65} &= -\frac{1}{4}\Big(-12 E_a^{'} G_1^{'} G_a^{'} b h_1 h_a^2 \nu_a^{'} + 12 E_a^{'} G_2^{'} G_a^{'} b h_2 h_a^2 \nu_a^{'} - 12 G_1^{'} G_a^{'2} b h_1 h_a^2 \\
&\quad +12 G_2^{'} G_a^{'2} b h_2 h_a^2\Big) \\
a_{66} &= -\frac{1}{4}\Big(600 E_a^{'} G_1^{'} G_2^{'} b h_1 h_2 h_a \nu_a^{'} + 41 E_a^{'} G_1^{'} G_a^{'} b h_1 h_a^2 \nu_a^{'} + 89 E_a^{'} G_2^{'} G_a^{'} b h_2 h_a^2 \nu_a^{'} \\
&\quad +5 E_a^{'} G_a^{'2} b h_a^3 \nu_a^{'} + 600 G_1^{'} G_2^{'} G_a^{'} b h_1 h_2 h_a + 41 G_1^{'} G_a^{'2} b h_1 h_a^2 + 29 G_2^{'} G_a^{'2} b h_2 h_a^2 \\
&\quad +2 G_a^{'3} b h_a^3\Big) \\
a_{67} &= -\frac{1}{4}\Big(-600 E_a^{'} G_1^{'} G_2^{'} b h_1^2 h_2 h_a \nu_a^{'} - 41 E_a^{'} G_1^{'} G_a^{'} b h_1^2 h_a^2 \nu_a^{'} - 89 E_a^{'} G_2^{'} G_a^{'} b h_1 h_2 h_a^2 \nu_a^{'} \\
&\quad -5 E_a^{'} G_a^{'2} b h_1 h_a^3 \nu_a^{'} - 600 G_1^{'} G_2^{'} G_a^{'} b h_1^2 h_2 h_a - 120 G_1^{'} G_2^{'} G_a^{'} b h_1 h_2 h_a^2 \\
&\quad -41 G_1^{'} G_a^{'2} b h_1^2 h_a^2 - 6 G_1^{'} G_a^{'2} b h_1 h_a^3 - 29 G_2^{'} G_a^{'2} b h_1 h_2 h_a^2 - 2 G_a^{'3} b h_1 h_a^3\Big) \\
a_{68} &= -\frac{1}{4}\Big(-600 E_a^{'} G_1^{'} G_2^{'} b h_1 h_2 h_a \nu_a^{'} - 89 E_a^{'} G_1^{'} G_a^{'} b h_1 h_a^2 \nu_a^{'} - 41 E_a^{'} G_2^{'} G_a^{'} b h_2 h_a^2 \nu_a^{'} \\
&\quad -5 E_a^{'} G_a^{'2} b h_a^3 \nu_a^{'} - 600 G_1^{'} G_2^{'} G_a^{'} b h_1 h_2 h_a - 29 G_1^{'} G_a^{'2} b h_1 h_a^2 - 41 G_2^{'} G_a^{'2} b h_2 h_a^2 \\
&\quad -2 G_a^{'3} b h_a^3\Big) \\
a_{69} &= -\frac{1}{4}\Big(-600 E_a^{'} G_1^{'} G_2^{'} b h_1 h_2^2 h_a \nu_a^{'} - 89 E_a^{'} G_1^{'} G_a^{'} b h_1 h_2 h_a^2 \nu_a^{'} - 41 E_a^{'} G_2^{'} G_a^{'} b h_2^2 h_a^2 \nu_a^{'} \\
&\quad -5 E_a^{'} G_a^{'2} b h_2 h_a^3 \nu_a^{'} - 600 G_1^{'} G_2^{'} G_a^{'} b h_1 h_2^2 h_a - 120 G_1^{'} G_2^{'} G_a^{'} b h_1 h_2 h_a^2 \\
&\quad -29 G_1^{'} G_a^{'2} b h_1 h_2 h_a^2 - 41 G_2^{'} G_a^{'2} b h_2^2 h_a^2 - 6 G_2^{'} G_a^{'2} b h_2 h_a^3 - 2 G_a^{'3} b h_2 h_a^3\Big)
\end{aligned}
\tag{A.10}
$$

$$
\begin{aligned}
a_{70} &= h_a^3 G_a^{'} b \left(240 G_1^{'} G_2^{'} h_1 h_2 + 16 G_1^{'} G_a^{'} h_1 h_a + 16 G_2^{'} G_a^{'} h_2 h_a + G_a^{'2} h_a^2\right) \\
a_{71} &= \frac{1}{4}\left(-300 E_a^{'} G_1^{'} G_a^{'} b h_1 h_a + 300 E_a^{'} G_2^{'} G_a^{'} b h_2 h_a\right) \\
a_{72} &= \frac{1}{4}\Big(10080 E_a^{'} G_1^{'} G_2^{'} b h_1 h_2 h_a + 924 E_a^{'} G_1^{'} G_a^{'} b h_1 h_a^2 + 924 E_a^{'} G_2^{'} G_a^{'} b h_2 h_a^2 \\
&\quad + 84 E_a^{'} G_a^{'2} b h_a^3\Big) \\
a_{73} &= \frac{1}{4}\Big(-5040 E_a^{'} G_1^{'} G_2^{'} b h_1 h_2 - 402 E_a^{'} G_1^{'} G_a^{'} b h_1 h_a - 702 E_a^{'} G_2^{'} G_a^{'} b h_2 h_a \\
&\quad - 57 E_a^{'} G_a^{'2} b h_a^2\Big) \\
a_{74} &= \frac{1}{4}\Big(5040 E_a^{'} G_1^{'} G_2^{'} b h_1 h_2 + 702 E_a^{'} G_1^{'} G_a^{'} b h_1 h_a + 402 E_a^{'} G_2^{'} G_a^{'} b h_2 h_a \\
&\quad + 57 E_a^{'} G_a^{'2} b h_a^2\Big) \\
a_{75} &= \frac{1}{4}\Big(3360 E_a^{'} G_1^{'} G_2^{'} b h_1 h_2 h_a \nu_a^{'} + 188 E_a^{'} G_1^{'} G_a^{'} b h_1 h_a^2 \nu_a^{'} + 188 E_a^{'} G_2^{'} G_a^{'} b h_2 h_a^2 \nu_a^{'} \\
&\quad + 8 E_a^{'} G_a^{'2} b h_a^3 \nu_a^{'} + 3360 G_1^{'} G_2^{'} G_a^{'} b h_1 h_2 h_a + 188 G_1^{'} G_a^{'2} b h_1 h_a^2 + 188 G_2^{'} G_a^{'2} b h_2 h_a^2 \\
&\quad + 8 G_a^{'3} b h_a^3\Big) \\
a_{76} &= \frac{1}{4}\Big(-1680 E_a^{'} G_1^{'} G_2^{'} b h_1 h_2 h_a \nu_a^{'} - 109 E_a^{'} G_1^{'} G_a^{'} b h_1 h_a^2 \nu_a^{'} - 259 E_a^{'} G_2^{'} G_a^{'} b h_2 h_a^2 \nu_a^{'} \\
&\quad - 19 E_a^{'} G_a^{'2} b h_a^3 \nu_a^{'} - 1680 G_1^{'} G_2^{'} G_a^{'} b h_1 h_2 h_a - 109 G_1^{'} G_a^{'2} b h_1 h_a^2 - 79 G_2^{'} G_a^{'2} b h_2 h_a^2 \\
&\quad - 4 G_a^{'3} b h_a^3\Big) \\
a_{77} &= \frac{1}{4}\Big(1680 E_a^{'} G_1^{'} G_2^{'} b h_1^2 h_2 h_a \nu_a^{'} + 109 E_a^{'} G_1^{'} G_a^{'} b h_1^2 h_a^2 \nu_a^{'} + 259 E_a^{'} G_2^{'} G_a^{'} b h_1 h_2 h_a^2 \nu_a^{'} \\
&\quad + 19 E_a^{'} G_a^{'2} b h_1 h_a^3 \nu_a^{'} + 1680 G_1^{'} G_2^{'} G_a^{'} b h_1^2 h_2 h_a + 360 G_1^{'} G_2^{'} G_a^{'} b h_1 h_2 h_a^2 \\
&\quad + 109 G_1^{'} G_a^{'2} b h_1^2 h_a^2 + 30 G_1^{'} G_a^{'2} b h_1 h_a^3 + 79 G_2^{'} G_a^{'2} b h_1 h_2 h_a^2 + 4 G_a^{'3} b h_1 h_a^3\Big) \\
a_{78} &= \frac{1}{4}\Big(-1680 E_a^{'} G_1^{'} G_2^{'} b h_1 h_2 h_a \nu_a^{'} - 259 E_a^{'} G_1^{'} G_a^{'} b h_1 h_a^2 \nu_a^{'} - 109 E_a^{'} G_2^{'} G_a^{'} b h_2 h_a^2 \nu_a^{'} \\
&\quad - 19 E_a^{'} G_a^{'2} b h_a^3 \nu_a^{'} - 1680 G_1^{'} G_2^{'} G_a^{'} b h_1 h_2 h_a - 79 G_1^{'} G_a^{'2} b h_1 h_a^2 - 109 G_2^{'} G_a^{'2} b h_2 h_a^2 \\
&\quad - 4 G_a^{'3} b h_a^3\Big) \\
a_{79} &= \frac{1}{4}\Big(-1680 E_a^{'} G_1^{'} G_2^{'} b h_1 h_2^2 h_a \nu_a^{'} - 259 E_a^{'} G_1^{'} G_a^{'} b h_1 h_2 h_a^2 \nu_a^{'} - 109 E_a^{'} G_2^{'} G_a^{'} b h_2^2 h_a^2 \nu_a^{'} \\
&\quad - 19 E_a^{'} G_a^{'2} b h_2 h_a^3 \nu_a^{'} - 1680 G_1^{'} G_2^{'} G_a^{'} b h_1 h_2^2 h_a - 360 G_1^{'} G_2^{'} G_a^{'} b h_1 h_2 h_a^2 \\
&\quad - 79 G_1^{'} G_a^{'2} b h_1 h_2 h_a^2 - 109 G_2^{'} G_a^{'2} b h_2^2 h_a^2 - 30 G_2^{'} G_a^{'2} b h_2 h_a^3 - 4 G_a^{'3} b h_2 h_a^3\Big)
\end{aligned}
\tag{A.11}
$$

$$
\begin{aligned}
a_{80} &= h_a b\left(240G_1^{'}G_2^{'}h_1h_2 + 16G_1^{'}G_a^{'}h_1h_a + 16G_2^{'}G_a^{'}h_2h_a + G_a^{'2}h_a^2\right)\\
a_{81} &= -\frac{1}{2}\left(400E_a^{'}G_2^{'}bh_2 + 20E_a^{'}G_a^{'}bh_a\right)\\
a_{82} &= -\frac{1}{2}\left(336E_a^{'}G_2^{'}bh_2h_a + 28E_a^{'}G_a^{'}bh_a^2\right)\\
a_{83} &= -\frac{1}{2}\left(-488E_a^{'}G_2^{'}bh_2 - 34E_a^{'}G_a^{'}bh_a\right)\\
a_{84} &= -\frac{1}{2}\left(88E_a^{'}G_2^{'}bh_2 + 14E_a^{'}G_a^{'}bh_a\right)\\
a_{85} &= -\frac{1}{2}\left(-48E_a^{'}G_2^{'}bh_2h_a\nu_a^{'} - 4E_a^{'}G_a^{'}bh_a^2\nu_a^{'} - 48G_2^{'}G_a^{'}bh_2h_a - 4G_a^{'2}bh_a^2\right)\\
a_{86} &= -\frac{1}{2}\left(-196E_a^{'}G_2^{'}bh_2h_a\nu_a^{'} - 13E_a^{'}G_a^{'}bh_a^2\nu_a^{'} + 44G_2^{'}G_a^{'}bh_2h_a + 3G_a^{'2}bh_a^2\right)\\
a_{87} &= -\frac{1}{2}\left(196E_a^{'}G_2^{'}bh_1h_2h_a\nu_a^{'} + 13E_a^{'}G_a^{'}bh_1h_a^2\nu_a^{'} + 480G_1^{'}G_2^{'}bh_1h_2h_a\right.\\
&\quad \left.+32G_1^{'}G_a^{'}bh_1h_a^2 - 44G_2^{'}G_a^{'}bh_1h_2h_a - 3G_a^{'2}bh_1h_a^2\right)\\
a_{88} &= -\frac{1}{2}\left(4E_a^{'}G_2^{'}bh_2h_a\nu_a^{'} - 3E_a^{'}G_a^{'}bh_a^2\nu_a^{'} + 4G_2^{'}G_a^{'}bh_2h_a + G_a^{'2}bh_a^2\right)\\
a_{89} &= -\frac{1}{2}\left(4E_a^{'}G_2^{'}bh_2^2h_a\nu_a^{'} - 3E_a^{'}G_a^{'}bh_2h_a^2\nu_a^{'} + 4G_2^{'}G_a^{'}bh_2^2h_a\right.\\
&\quad \left.-8G_2^{'}G_a^{'}bh_2h_a^2 + G_a^{'2}bh_2h_a^2\right)
\end{aligned}
\tag{A.12}
$$

$$
\begin{aligned}
a_{90} &= h_a b \left(240 G_1^{'} G_2^{'} h_1 h_2 + 16 G_1^{'} G_a^{'} h_1 h_a + 16 G_2^{'} G_a^{'} h_2 h_a + G_a^{'2} h_a^2\right) \\
a_{91} &= \frac{1}{2}\left(-400 E_a^{'} G_1^{'} b h_1 - 20 E_a^{'} G_a^{'} b h_a\right) \\
a_{92} &= \frac{1}{2}\left(336 E_a^{'} G_1^{'} b h_1 h_a + 28 E_a^{'} G_a^{'} b h_a^2\right) \\
a_{93} &= \frac{1}{2}\left(-88 E_a^{'} G_1^{'} b h_1 - 14 E_a^{'} G_a^{'} b h_a\right) \\
a_{94} &= \frac{1}{2}\left(488 E_a^{'} G_1^{'} b h_1 + 34 E_a^{'} G_a^{'} b h_a\right) \\
a_{95} &= \frac{1}{2}\left(-48 E_a^{'} G_1^{'} b h_1 h_a \nu_a^{'} - 4 E_a^{'} G_a^{'} b h_a^2 \nu_a^{'} - 48 G_1^{'} G_a^{'} b h_1 h_a - 4 G_a^{'2} b h_a^2\right) \\
a_{96} &= \frac{1}{2}\left(4 E_a^{'} G_1^{'} b h_1 h_a \nu_a^{'} - 3 E_a^{'} G_a^{'} b h_a^2 \nu_a^{'} + 4 G_1^{'} G_a^{'} b h_1 h_a + G_a^{'2} b h_a^2\right) \\
a_{97} &= \frac{1}{2}\Big(-4 E_a^{'} G_1^{'} b h_1^2 h_a \nu_a^{'} + 3 E_a^{'} G_a^{'} b h_1 h_a^2 \nu_a^{'} - 4 G_1^{'} G_a^{'} b h_1^2 h_a \\
&\quad + 8 G_1^{'} G_a^{'} b h_1 h_a^2 - G_a^{'2} b h_1 h_a^2\Big) \\
a_{98} &= \frac{1}{2}\left(-196 E_a^{'} G_1^{'} b h_1 h_a \nu_a^{'} - 13 E_a^{'} G_a^{'} b h_a^2 \nu_a^{'} + 44 G_1^{'} G_a^{'} b h_1 h_a + 3 G_a^{'2} b h_a^2\right) \\
a_{99} &= \frac{1}{2}\Big(-196 E_a^{'} G_1^{'} b h_1 h_2 h_a \nu_a^{'} - 13 E_a^{'} G_a^{'} b h_2 h_a^2 \nu_a^{'} - 480 G_1^{'} G_2^{'} b h_1 h_2 h_a \\
&\quad + 44 G_1^{'} G_a^{'} b h_1 h_2 h_a - 32 G_2^{'} G_a^{'} b h_2 h_a^2 + 3 G_a^{'2} b h_2 h_a^2\Big)
\end{aligned}
\tag{A.13}
$$

References

[1] T. H. Nguyen, P. Le Grognec, Analytical and numerical simplified modeling of a single-lap joint, International Journal of Adhesion and Adhesives 108 (2021) 102827. doi:10.1016/j.ijadhadh.2021.102827.

[2] T. Methfessel, W. Becker, A generalized model for predicting stress distributions in thick adhesive joints using a higher-order displacement approach, Composite Structures 291 (2022) 115556. doi:10.1016/j.compstruct.2022.115556.

[3] I. Arnovljevic, Das Verteilungsgesetz der Haftspannung bei axial beanspruchten Verbundstaben, Zeitschrift fur Architektur und Ingenieurwesen 2 (1909) 413–418.

[4] O. Volkersen, Die Nietkraftverteilung in Zugbeanspruchten Nietverbindungen mit konstanten Laschenquerschnitten, Luftfahrtforschung 15 (24) (1938) 41–47.

[5] M. Goland, E. Reissner, The stresses in cemented joints, Journal of Applied Mechanics 11 (1944) A17–A27.

[6] L. Hart-Smith, Adhesive bonded single lap joints, NASA Technical Report CR112236, Douglas Aircraft Company, Long Beach (1973).

[7] I. U. Ojalvo, H. L. Eidinoff, Bond Thickness Effects upon Stresses in Single-Lap Adhesive Joints, AIAA Journal 16 (3) (1978) 204–211. doi:10.2514/3.60878.

[8] D. Oplinger, A Layered Beam Theory for Single-Lap Joints, US AMTL Technical Report MTL91-23, US Army Materials Technology Laboratory (1991).

[9] Q. Luo, L. Tong, Fully-coupled nonlinear analysis of single lap adhesive joints, International Journal of Solids and Structures 44 (7-8) (2007) 2349–2370. doi:10.1016/j.ijsolstr.2006.07.009.

[10] Q. Luo, L. Tong, Analytical solutions for adhesive composite joints considering large deflection and transverse shear deformation in adherends, International Journal of Solids and Structures 45 (22-23) (2008) 5914–5935. doi:10.1016/j.ijsolstr.2008.07.001.

[11] Q. Luo, L. Tong, Analytical solutions for nonlinear analysis of composite single-lap adhesive joints, International Journal of Adhesion and Adhesives 29 (2) (2009) 144–154. doi:10.1016/j.ijadhadh.2008.01.007.

[12] J. H. Williams, Stresses in Adhesive between Dissimilar Adherends, The Journal of Adhesion 7 (2) (1975) 97–107. doi:10.1080/00218467508075042.

[13] D. Bigwood, A. Crocombe, Elastic analysis and engineering design formulae for bonded joints, International Journal of Adhesion and Adhesives 9 (4) (1989) 229–242. doi:10.1016/0143-7496(89)90066-3.

[14] K. Alfredsson, J. Högberg, A closed-form solution to statically indeterminate adhesive joint problems—exemplified on ELS-specimens, International Journal of Adhesion and Adhesives 28 (7) (2008) 350–361. doi:10.1016/j.ijadhadh.2007.10.002.

[15] J. Wang, C. Zhang, Three-parameter, elastic foundation model for analysis of adhesively bonded joints, International Journal of Adhesion and Adhesives 29 (5) (2009) 495–502. doi:10.1016/j.ijadhadh.2008.10.002.

[16] P. Weißgraeber, N. Stein, W. Becker, A general sandwich-type model for adhesive joints with composite adherends, International Journal of Adhesion and Adhesives 55 (2014) 56–63. doi:10.1016/j.ijadhadh.2014.06.009.

[17] B. Zhao, Z.-H. Lu, Y.-N. Lu, Closed-form solutions for elastic stress–strain analysis in unbalanced adhesive single-lap joints considering adherend deformations and bond thickness, International Journal of Adhesion and Adhesives 31 (6) (2011) 434–445. doi:10.1016/j.ijadhadh.2011.03.002.

[18] F. Mortensen, O. T. Thomsen, Simplified linear and non-linear analysis of stepped and scarfed adhesive-bonded lap-joints between composite laminates, Composite Structures 38 (1) (1997) 281–294. doi:10.1016/S0263-8223(97)00063-9.

[19] F. Mortensen, O. Thomsen, Analysis of adhesive bonded joints: a unified approach, Composites Science and Technology 62 (7-8) (2002) 1011–1031. doi:10.1016/S0266-3538(02)00030-1.

[20] E. Paroissien, M. Sartor, J. Huet, F. Lachaud, Analytical Two-Dimensional Model of a Hybrid (Bolted/Bonded) Single-Lap Joint, Journal of Aircraft 44 (2) (2007) 573–582. doi:10.2514/1.24452.

[21] E. Paroissien, F. Lachaud, S. Schwartz, Modelling load transfer in single-lap adhesively bonded and hybrid (bolted / bonded) joints, Progress in Aerospace Sciences 130 (2022) 100811. doi:10.1016/j.paerosci.2022.100811.

[22] D. Chen, S. Cheng, An Analysis of Adhesive-Bonded Single-Lap Joints, Journal of Applied Mechanics 50 (1) (1983) 109–115. doi:10.1115/1.3166976.

[23] Y. Gilibert, A. Rigolot, Théorie élastique de l'assemblage collé à double recouvrement: utilisation de la méthode des développements asymptotiques raccordés au voisinage des extrémités, Materials and Structures 18 (5) (1985) 363–387. doi:10.1007/BF02472407.

[24] F. Chen, P. Qiao, On the intralaminar and interlaminar stress analysis of adhesive joints in plated beams, International Journal of Adhesion and Adhesives 36 (2012) 44–55. doi:10.1016/j.ijadhadh.2012.03.005.

[25] W. Jiang, P. Qiao, An improved four-parameter model with consideration of Poisson's effect on stress analysis of adhesive joints, Engineering Structures 88 (2015) 203–215. doi:10.1016/j.engstruct.2015.01.027.

[26] D. J. Allman, A THEORY FOR ELASTIC STRESSES IN ADHESIVE BONDED LAP JOINTS, The Quarterly Journal of Mechanics and Applied Mathematics 30 (4) (1977) 415–436. doi:10.1093/qjmam/30.4.415.

[27] R. D. Adams, V. Mallick, A Method for the Stress Analysis of Lap Joints, The Journal of Adhesion 38 (3-4) (1992) 199–217. doi:10.1080/00218469208030455.

[28] E. Paroissien, A. Da Veiga, A. Laborde, An 1D-Beam Approach for Both Stress Analysis and Fatigue Life Prediction of Bonded Joints, in: J. Komorowski (Ed.), ICAF 2011 Structural Integrity: Influence of Efficiency and Green Imperatives, Springer Netherlands, Dordrecht, 2011, pp. 359–374. doi:10.1007/978-94-007-1664-3_29.

[29] S. Schwartz, E. Paroissien, F. Lachaud, General formulation of macro-elements for the simulation of multi-layered bonded structures, The Journal of Adhesion 96 (6) (2020) 602–632. doi:10.1080/00218464.2019.1622420.

[30] B. Ordonneau, E. Paroissien, M. Salaün, J. Malrieu, A. Guigue, S. Schwartz, A methodology for the computation of the macro-element stiffness matrix for the stress analysis of a lap joint with functionally graded adhesive properties, International Journal of Adhesion and Adhesives 97 (2020) 102505. doi:10.1016/j.ijadhadh.2019.102505.

[31] C. D. C. D. Maia, W. K. F. Brito, A. V. Mendonca, A static boundary element solution for Bickford–Reddy beam, Engineering with Computers 36 (4) (2020) 1435–1451. doi:10.1007/s00366-019-00774-5.

[32] G. Lelias, E. Paroissien, F. Lachaud, J. Morlier, S. Schwartz, C. Gavoille, An extended semi-analytical formulation for fast and reliable mode I/II stress analysis of adhesively bonded joints, International Journal of Solids and Structures 62 (2015) 18–38. doi:10.1016/j.ijsolstr.2014.12.027.

[33] E. Paroissien, F. Lachaud, L. F. da Silva, S. Seddiki, A comparison between macro-element and finite element solutions for the stress analysis of functionally graded single-lap joints, Composite Structures 215 (2019) 331–350. doi:10.1016/j.compstruct.2019.02.070.